N-71-16802

PREDICTION OF THE DYNAMIC ENVIRONMENT OF SPACECRAFT COMPONENTS

Part II. Acoustic and Structural Path Transmission Through Two Models of a Shroud-Enclosed Spacecraft

Joshua E. Greenspon

National Aeronautics and Space Administration
Goddard Space Flight Center
Contract NAS 5-10180
Final Report
October, 1970

Attn: Mr. Joseph Young, Code 321

J G ENGINEERING RESEARCH ASSOCIATES

3831 MENLO DRIVE   BALTIMORE 15, MARYLAND

1. Report No.	2. Government Accession No.	3. Recipient's Catalog No.
4. Title and Subtitle See Abstract below		5. Report Date October, 1970
		6. Performing Organization Code
7. Author(s) Joshua E. Greenspon		8. Performing Organization Report No.
9. Performing Organization Name and Address J G ENGINEERING RESEARCH ASSOCIATES 3831 Menlo Drive Balto., Md. 21215		10. Work Unit No.
		11. Contract or Grant No. NAS 5-10180
		13. Type of Report and Period Covered
12. Sponsoring Agency Name and Address Goddard Space Flight Center Greenbelt, Maryland 20771		Final Report October, 1970
		14. Sponsoring Agency Code 321

15. Supplementary Notes

16. Abstract

Prediction of the Dynamic
Environment of Spacecraft
Components-Part II. Acoustic
and Structural Path Transmission
Through Two Models of
a Shroud-Enclosed Spacecraft

This report treats the structural path and acoustic path
transmission of an unstiffened and stiffened shroud with
spacecraft boxes contained within the shroud. The modes
and frequencies of both systems were determined from a
finite element program. The low frequency region below
640 cps is treated. It is found that there is not much
difference in the structural path transmission between
the two configurations, whereas as the acoustic trans-
mission of the unstiffened shroud is an order of
magnitude greater than the stiffened shroud

17. Key Words (Selected by Author(s))	18. Distribution Statement

19. Security Classif. (of this report) UNCLASSIFIED	20. Security Classif. (of this page) UNCLASSIFIED	21. No. of Pages 37	22. Price*

ABSTRACT

This report treats the structural path and acoustic path transmission of an unstiffened and stiffened shroud with spacecraft boxes contained within the shroud. The modes and frequencies of both systems were determined from a finite element program. The low frequency region below 640 cps is treated. It is found that there is not much difference in the structural path transmission between the two configurations, whereas the acoustic transmission of the unstiffened shroud is an order of magnitude greater than that of the stiffened shroud.

TABLE OF CONTENTS

ACKNOWLEDGEMENTS

LIST OF SYMBOLS

$\eta_j(t)$	Displacement at point j at time t
z_{jm}	Value of the mth mode shape at point j of the structure
$q_m(t)$	Generalized coordinate for the mth mode
$Q_m(t)$	Generalized force for the mth mode
β_m	Ratio of damping to critical damping for the mth mode
ω_m	Natural frequency of the mth mode (in radian measure)
z_{rm}	Value of the mth mode shape at point r of the structure
$P_r(t)$	Applied load per unit area at point r at time t
A_r	Area over which the applied load Pr(t) acts
Ω	Spectral frequency (i.e. the frequency of the exciting forces)
$q_m(\Omega)$	Fourier transform of qm(t)
$Q_m(\Omega)$	Fourier transform of Qm(t)
$\eta_{jk}(\Omega)$	Cross spectrum of the displacements at points j and k at frequency Ω
$\eta_j^*(\Omega)$	Complex conjugate of $\eta_j(\Omega)$
$Y_m(\Omega)$	Modal frequency response function for the mth mode
$P_{rs}(\Omega)$	Cross spectrum of the exciting pressures at points r and s at frequency Ω
$\Delta\Omega$	Frequency band over which the RMS value is desired
$\eta_j(RMS)$	Root mean square displacement at point j over frequency band $\Delta\Omega$
$a_j(RMS)$	Root mean square acceleration at point j over frequency band $\Delta\Omega$
$C_{mm}(\Omega)$	Joint acceptance (or generalized force for random loading)-mth mode
$P_0(\omega)$	Spectrum of the applied outside pressure to the shroud
ξ	$|z_1 - z_2|$ or $a|\phi_1 - \phi_2|$ difference in the coordinate values in a homogeneous correlation function
k	$\omega/c_0 = \Omega/c_0$
ω	Forcing or spectral frequency of the applied pressure $(=\Omega)$
c_0	Sound velocity in the medium outside the shroud
α, β	Constants used to describe the exponentially decaying correction function
$J_0(k\xi)$	Zeroth order Bessel Function with argument $k\xi$

M_m	Modal mass for mth mode of structure
$A = A_{Shroud}$	shroud surface area
A_c	Correlation area
J_{mm}^2	Powell's joint acceptance for the mth mode
z, ϕ	Cylindrical coordinates for the shell
$\bar{C}_{mm}(\omega) = C_{mm}(\omega)/p_o(\omega)$	
$w(z, \phi, t)$	Radial displacement on the surface of a cylindrical shell at cylindrical coordinates z, ϕ at time t
$N_{\bar{m}\bar{n}}(t), U_{\bar{m}\bar{n}}(t)$	Fourier component displacements of the cylindrical shell
$\bar{m}, \bar{p}$	For the cylindrical shell (shroud) this is the number of axial half waves in the vibration pattern of the shroud
$\bar{p}(z, \phi, t)$	Pressure applied to the shroud
$f_{\bar{m}\bar{n}}(t), g_{\bar{m}\bar{n}}(t)$	Fourier component pressure functions for the shroud
h_w, h_w	Modal impulse functions for the shell (shroud)
H_w, K_w	Modal frequency response functions for the shell (shroud)
$\bar{w}(z_1, \phi_1, z_2, \phi_2, \omega)$	Cross spectrum of displacement at point x_1, ϕ_1 with displacement at x_2, ϕ_2 at frequency ω
$\bar{\xi}_1, \bar{\xi}_2$	Variables of integration in the Z direction
$\bar{\eta}_1, \bar{\eta}_2$	Variable of integration in the ϕ direction
$[\bar{P}_i(r, \omega)]_{Ave.}$	Space average spectrum of the pressure over the inside of the shroud at radial distance r from the shroud axis
H_{p_i}	Frequency response function for acoustic pressure inside the shroud
ν	Poisson's ratio for shell (shroud) material
h	Cylinder (shroud) thickness
a	Cylinder (shroud) radius
c_i	Sound velocity in air inside shroud
ρ	Mass density of shell (shroud) material
ρ_i	Density of the air inside the shroud
$I_{\bar{n}}, J_{\bar{n}}$	Bessel Functions of order $\bar{n}$ of imaginary and real arguments
ℓ	Length of the shell (shroud)
$\gamma_{\bar{m}\bar{n}}$	Acoustic pressure function of the mnth mode for the inside of the shroud
$\bar{n}, \bar{q}$	number of circumferential waves in the vibration pattern of the shell (shroud)

E Modulus of elasticity of shell material

$\omega_{\bar{m}\bar{n}}$ Natural frequency of the $\bar{m}\bar{n}$th mode of the shell

$\mathcal{S}$ Ratio of damping to critical damping

T_{sy} Nondimensional displacement transfer function

T_{sa} Nondimensional acceleration transfer function

I. Introduction

The first part of this study[1*] was completed the latter part of 1965. The earlier report[1] contained the basic theory for obtaining the structural and acoustic response of a shroud-spacecraft combination under random loading. As a continuation of the study the basic theory has been amended and applied to two models which resemble the OGO shroud-spacecraft combination. The results of the calculations are contained in this report.

II. Structural Response Relations

A. General Relations

The total displacement $\eta_j(t)$ of a structure at point j at time t can be written in terms of the displacements in each of its m modes of vibration as follows:

$$\eta_j(t) = \sum_m Z_{jm} q_m(t) \qquad [1]$$

where m is the mode number, Z_{jm} is the value of the mth mode shape at point j, $q_m(t)$ is a function of time which satisfies the following equation:

$$\ddot{q}_m(t) + 2\beta_m \omega_m \dot{q}_m(t) + \omega_m^2 q_m(t) = Q_m(t) \qquad [2]$$

in which β_m is the damping ratio (ratio of damping to critical damping) in the mth mode, ω_m is the undamped natural frequency of the mth mode and Qm(t) is the generalized force for the mth mode. Qm(t) can be written in terms of the loading P(t) as follows:

$$Q_m(t) = \sum_r Z_{rm} A_r P_r(t) \qquad [3]$$

where Z_{rm} is the value of the mth mode shape at point r, Ar is the area over which Pr(t) acts, and Pr(t) is the pressure at point r on the structure. Z_{rm} is the component of the mth mode shape in the direction of the load at point r.

Take the Fourier Transform of eq. [2] and denote the Fourier Transform of qm(t) by qm (Ω), then

$$\left[-\Omega^2 + i\, 2\beta_m \omega_m \Omega + \omega_m^2 \right] q_m(\Omega) = Q_m(\Omega) \qquad [4]$$

The cross spectrum between the displacements at point j and k is defined as

$$\eta_{jk}(\Omega) = \lim_{T \to \infty} \frac{\eta_k(\Omega)\, \eta_j^*(\Omega)}{T} \qquad [5]$$

(η_j^* being the complex conjugate of η_j)

---

*Superscripts refer to references listed at the end of the report.

-1-

but

$$\eta_j(\Omega) = \sum_m Z_{jm} \, q_m(\Omega) \qquad [6]$$

$$Q_m(\Omega) = \sum_r Z_{rm} \, A_r \, P_r(\Omega) \qquad [7]$$

So

$$\eta_j(\Omega) = \sum_m Z_{jm} \, Q_m(\Omega) \, Y_m(\Omega) \qquad [8]$$

$$= \sum_m Z_{jm} \, Y_m \sum_r Z_{rm} \, A_r \, P_r(\Omega)$$

Thus

$$\eta_{jk}(\Omega) = \sum_m \sum_n Z_{jm} \, Z_{kn} \, Y_m^*(\Omega) \, Y_n(\Omega) \, C_{mn}(\Omega) \qquad [9]$$

where

$$C_{mn}(\Omega) = \sum_r \sum_s Z_{rm} \, Z_{sn} \, P_{rs}(\Omega) \, A_r A_s \qquad [10]$$

$$P_{rs}(\Omega) = \lim_{T \to \infty} \frac{P_r^*(\Omega) \, P_s(\Omega)}{T} \qquad [11]$$

$$Y_m(\Omega) = \frac{1}{\omega_m^2 - \Omega^2 + i 2 \beta_m \omega_m \Omega}$$

Ym* is the complex conjugate of Ym, Prs (Ω) is the cross spectrum of the loading at points r and s.

It should be noted that Zrm and Zsm are the mode shape components in the direction of the loading at points r and s, and Zjm, Zkm are the mode shape components in any desired direction at each of the points j and k for which the cross spectrum is desired.

The RMS value of the deflection at j over a frequency band $\Delta\Omega = \Omega_{max} - \Omega_{min}$ can be written

$$\eta_j(RMS) = \left[\frac{1}{2\pi} \int_{\Omega_{min}}^{\Omega_{max}} \eta_{jj}(\Omega) \, d\Omega \right]^{1/2} \qquad [12]$$

where $\eta_{jj}(\Omega)$ is the auto spectrum of the displacement at point j and at frequency Ω.

If damping is small (as it will be in the models which we are considering in this report) then cross product terms can be neglected in equations [9] and [10] and they reduce to

$$\eta_{jk}(\Omega) = \sum_m Z_{jm} \, Z_{km} \, |Y_m(\Omega)|^2 \, C_{mm}(\Omega) \qquad [13]$$

where

$$C_{mm}(\Omega) = \sum_r \sum_s Z_{rm} \, Z_{sm} \, P_{rs}(\Omega) \, A_r A_s \qquad [14]$$

The auto spectrum of the displacement at point j can be written

$$\eta_{jj}(\Omega) = \sum_m Z_{jm}^2 \, |Y_m(\Omega)|^2 \, C_{mm}(\Omega) \qquad [15]$$

The RMS value of displacement can then be written

$$\eta_j(RMS) = \sum_m \left[\frac{1}{2\pi} \left(\int_{\Omega_1}^{\Omega_2} C_{mm}(\Omega) \, |Y_m(\Omega)|^2 \, d\Omega \right) Z_{jm}^2 \right]^{1/2} \qquad [16]$$

-2-

For cases of light damping this equation can be integrated to yield[2] (noting that for most practical cases $C_{mm}(\Omega)$ is approximately constant over the integration interval and can therefore be taken outside the integral)

$$\eta_j(RMS) = \left[\sum_m \frac{C_{mm}(\omega_m) \bar{Z}_{jm}^2}{8 \beta_m \omega_m^3} \right]^{1/2} \tag{17}$$

where the sum is taken over those modes which have their resonances in the band Ω_1 to Ω_2. Since the spectrum of acceleration is $\Omega^4 \eta_{jj}(\Omega)$, the RMS acceleration can be written

$$a_j(RMS) = \left[\sum_m \frac{C_{mm}(\omega_m) \bar{Z}_{jm}^2 \omega_m}{8 \beta_m} \right]^{1/2} \tag{18}$$

Note that in all the above calculations the Zjm are the normalized mode shapes, i.e.

$$Z_{jm} = \sqrt{m_m} \, \bar{Z}_{jm} \tag{19}$$

where $\bar{Z}_{jm}$ are the unnormalized mode shapes.

B. Simplification of the Cmm(ω)

Let $C_{mm}(\omega) = P_o(\omega) \bar{C}_{mm}(\omega)$, where $p_o(\omega)$ is the auto spectrum of the input pressure. It has been shown by Powell[3] that for structures with sinusoidal mode shapes, such as simply supported plates, which are excited by random forces in which the cross spectrum falls to a small value in a distance which is small compared to the structural wave length then Cmm(ω) is not a function of the mode shape. Moreover Bozich[4] has determined Cmm for simply supported and fixed plates and has found that Cmm not only is a constant function of mode shape for correlations which display a sharp cut-off but it does not vary much with frequency. For a large number of practical cases the correlation will take one of the following forms:

$$G(\xi, \omega) = \frac{\sin k\xi}{k\xi} \tag{20a}$$

where $\xi = |z_1 - z_2|$ or

$$G(\xi, \omega) = J_o(k\xi) \tag{20b}$$

$$= a|\phi_1 - \phi_2|$$

$$G(\xi, \omega) = e^{-\alpha\xi} \cos\beta\xi \tag{20c}$$

in which z_1, z_2 are two longitudinal coordinates on a structure and ϕ_1, ϕ_2 are two peripheral coordinates.

For the unstiffened shroud shown in Figure 1, it was found that

$$\bar{C}_{mm}(\omega) \approx 2 \times 10^7 \quad \text{(in lb., inch, sec. units)} \tag{21}$$

The $\bar{C}_{mm}$ did not vary much with either frequency or mode shape. In the calculation of Cmm equation [20a] was used. Separate calculations of $G(\xi, \omega)$

from equation [20a] showed that it fell to a very small value (of the order of 10^{-4}) in a distance which was small compared to any of the modal wave lengths that are shown in Figures 2 - 8 and the other mode shapes used in the computations.

A list of Cmm(ω) are shown in Table 1.

Table 1   Cmm(ω) Values for Unstiffened Shroud

Frequency (cps)	Mode	Cmm (ω)
160	25	1.98×10^7
160	31	1.98×10^7
160	30	1.98×10^7
64	13	2.25×10^7
64	12	2.20×10^7
128	12	1.88×10^7
64	10	2.20×10^7
64	11	2.23×10^7
2000	32	1.79×10^7
20000	32	1.78×10^7

In terms of Powell's correlation area[3] and joint acceptance[3] the Cmm can be written as follows:

$$\bar{C}_{mm}(\omega) = j_{mm}^2 A^2 / M_m \qquad [22]$$

where

$$j_{mm}^2 = \frac{1}{4} \frac{A_c}{A} \qquad [23]$$

in which Ac = correlation area and A is the actual shroud area.

A list of the calculated jmm values is contained in Table 2 for the unstiffened shroud.

Table 2   Joint Acceptance Values – Unstiffened Shroud

Mode m	Mm	Cmm (ω)	Jmm^2
25	.0176	1.98×10^7	.0646
31	.0173	1.98×10^7	.0635
30	.0172	1.98×10^7	.0631
13	.0212	2.25×10^7	.0884
12	.0144	2.20×10^7	.0588
10	.0173	2.20×10^7	.0705
11	.0306	2.23×10^7	.1263

Using an average value of $jmm^2 \approx .08$ [23a] it is seen that

$$A_c/A \approx .3 \tag{24}$$

Thus the correlation area is of the order of 30% of the shroud area for those modes considered in the above calculations.

Based on the above calculations, an average value of $\frac{A_c}{A} \approx .3$ will be used in this analysis for both the unstiffened shroud shown in Figure 1 and the stiffened shroud shown in Figure 9. as well as for the acoustic loading for the spacecraft boxes on the inside of both shrouds.   Since only the low frequency behavior will be studied in detail in this report, it seems that this should be an adequate approximation to obtain order of magnitude results.

III. Acoustic transmission through the shroud

A. General relations

Both the stiffened and unstiffened shroud are cylindrical shells.   For purposes of the calculations of the acoustic field inside the shroud, it will be assumed that the shells have freely supported ends.   The general solution for the lateral displacement, w, of a shell with freely supported ends has been written down by Rattaya and Junger,[5] it is

$$w(z, \phi, t) = \sum_{n=0}^{\infty} \sum_{m=1}^{\infty} \left[V_{mn}(t) \cos n\phi + U_{mn}(t) \sin n\phi \right] \sin \frac{m\pi z}{\ell} \tag{25}$$

In this representation of the shell response it has been assumed that the general external loading has been decomposed into Fourier components as follows: (i.e. the loading has been expanded into a series of functions which are identical with the mode shape functions of the shell)

$$\bar{p}(z, \phi, t) = \sum_{n=0}^{\infty} \sum_{m=1}^{\infty} \left[f_{mn}(t) \cos n\phi + g_{mn}(t) \sin n\phi \right] \sin \frac{m\pi z}{\ell} \tag{26}$$

The Fourier coefficients of the loading are given by

*This is a particular solution which satisfies freely supported end conditions; it is the most general solution in ϕ but is particular in Z.

-5-

$$f_{\bar{m}\bar{n}}(t) = \frac{2}{\pi \ell} \int_0^\ell \int_0^{2\pi} \bar{p}(z,\phi,t) \cos \bar{n}\phi \sin \frac{\bar{m}\pi z}{\ell} \, dz \, d\phi$$

$$g_{\bar{m}\bar{n}}(t) = \frac{2}{\pi \ell} \int_0^\ell \int_0^{2\pi} \bar{p}(z,\phi,t) \sin \bar{n}\phi \sin \frac{\bar{m}\pi z}{\ell} \, dz \, d\phi \qquad [27]$$

The $v_{mn}(t)$ and $u_{mn}(t)$ can be written in terms of impulse functions h_w and k_w as follows:

$$v_{\bar{m}\bar{n}}(t) = \int_{-\infty}^{+\infty} f_{\bar{m}\bar{n}}(\theta) \, h_w(\bar{m},\bar{n},t-\theta) \, d\theta \qquad [28]$$

$$u_{mn}(t) = \int_{-\infty}^{+\infty} g_{\bar{m}\bar{n}}(\theta) \, k_w(\bar{m},\bar{n},t-\theta) \, d\theta$$

If the component loading has the form

$$\bar{p}_\ell(z,\phi,t) = \cos \bar{n}\phi \sin \frac{\bar{m}\pi z}{\ell} e^{i\omega t} \qquad [29]$$

The response will be

$$w_\ell(z,\phi,t) = H_w(\bar{m},\bar{n},\omega) e^{i\omega t} \sin \frac{\bar{m}\pi z}{\ell} \cos \bar{n}\phi \qquad [30]$$

and if the loading has the form

$$\bar{p}_\ell(z,\phi,t) = \sin \bar{n}\phi \sin \frac{\bar{m}\pi z}{\ell} e^{i\omega t} \qquad [31]$$

the response will be

$$w_\ell(z,\phi,t) = K_w(\bar{m},\bar{n},\omega) e^{i\omega t} \sin \frac{\bar{m}\pi z}{\ell} \sin \bar{n}\phi \qquad [32]$$

H_w and K_w are the complex frequency response functions for lateral displacement. They are Fourier Transforms of the impulse functions h_w and k_w respectively, i.e.

$$H_w(\bar{m},\bar{n},\omega) = \int_{-\infty}^{+\infty} h_w(\bar{m},\bar{n},t) e^{-i\omega t} \, dt \qquad [33]$$

The cross spectral density of the deflection, $\tilde{w}$, can be written (by definition)

$$\tilde{w}(z_1,\phi_1,z_2,\phi_2,\omega) = \frac{1}{2\pi} \int_{-\infty}^{+\infty} \langle w(x_1,\phi_1,t) w(z_2,\phi_2,t+\tau) \rangle e^{-i\omega\tau} \, d\tau \qquad [34]$$

where

$$\langle A \rangle = \lim_{T \to \infty} \frac{1}{2T} \int_{-T}^{+T} A \, dt$$

Using the previous relations

$$\tilde{w}(z_1,\phi_1,z_2,\phi_2,\omega) = \frac{1}{2\pi} \sum_{\bar{m}=1}^{\infty} \sum_{\bar{n}=0}^{\infty} \sum_{\bar{p}=1}^{\infty} \sum_{\bar{q}=0}^{\infty} \sin \frac{\bar{m}\pi z_1}{\ell} \sin \frac{\bar{p}\pi z_2}{\ell} \times \qquad [35]$$

$$\int_{-\infty}^{+\infty} \Big[\langle v_{\bar{m}\bar{n}}(t) v_{\bar{p}\bar{q}}(t+\tau) \rangle \cos \bar{n}\phi_1 \cos \bar{q}\phi_2$$

$$+ \langle u_{\bar{m}\bar{n}}(t) u_{\bar{p}\bar{q}}(t+\tau) \rangle \sin \bar{n}\phi_1 \sin \bar{q}\phi_2$$

$$+ \langle u_{\bar{m}\bar{n}}(t) v_{\bar{p}\bar{q}}(t+\tau) \rangle \sin \bar{n}\phi_1 \cos \bar{q}\phi_2$$

$$+ \langle v_{\bar{m}\bar{n}}(t) u_{\bar{p}\bar{q}}(t+\tau) \rangle \cos \bar{n}\phi_1 \sin \bar{q}\phi_2 \Big] e^{-i\omega\tau} \, d\tau$$

Now

$$I_1 = \int_{-\infty}^{+\infty} \langle v_{\bar{m}\bar{n}}(t) v_{\bar{p}\bar{q}}(t+\tau) \rangle e^{-i\omega\tau} \, d\tau = \int_{-\infty}^{+\infty} \left\{ \frac{1}{2T} \int_{-T}^{+T} \left[\int_{-\infty}^{+\infty} f_{\bar{m}\bar{n}}(\theta_1) h_w(\bar{m},\bar{n},t-\theta_1) d\theta_1 \right] \left[\int_{-\infty}^{+\infty} f_{\bar{p}\bar{q}}(\theta_2) h_w(\bar{p},\bar{q},t-\theta_2+\tau) d\theta_2 \right] dt \right\} e^{-i\omega\tau} d\tau$$

where $f_{\bar{m}\bar{n}}(\theta_1) = \frac{2}{\pi \ell} \int_0^\ell \int_0^{2\pi} \bar{p}(z,\phi,\theta_1) \cos \bar{n}\phi \sin \frac{\bar{m}\pi z}{\ell} \, dz \, d\phi$ $\qquad u_1 = t-\theta_1, \ u_2 = t-\theta_2+\tau$ $\qquad [36]$

We assume that the process is stationary so that the loading will be a function of the difference of the times θ_1, θ_2; let this difference be denoted by τ_3

-6-

$$\tau_3 = \theta_2 - \theta_1 = (t - u_2 + \tau) - (t - u_1) = u_1 - u_2 + \tau$$

then

$$\bar{I}_1 = \frac{4}{\pi^2 \ell^2} \int_0^\ell \sin \frac{\bar{m}\pi z_1}{\ell} dz_1 \int_0^\ell \sin \frac{\bar{p}\pi z_2}{\ell} dz_2 \int_0^{2\pi} \cos \bar{n}\phi_1 \, d\phi_1 \int_0^{2\pi} \cos \bar{q}\phi_2 \, d\phi_2 \times$$
$$\left\{ \int_{-\infty}^{+\infty} d\tau_3 \int_{-\infty}^{+\infty} du_1 \int_{-\infty}^{+\infty} du_2 \, h_w(\bar{m},\bar{n},u_1) h_w(\bar{p},\bar{q},u_2) e^{-iw(\tau_3 - u_1 + u_2)} \right.$$
$$\left. \left[\lim_{T\to\infty} \frac{1}{2T} \int_{-T}^{+T} \bar{p}(z_1,\phi_1, t-u_1)\, \bar{p}(z_2,\phi_2, t-u_2+\tau) \, dt \right] \right\} \qquad [37]$$

$$\bar{I}_1 = \frac{4}{\pi^2 \ell^2} \int_0^\ell \sin \frac{\bar{m}\pi z_1}{\ell} dz_1 \int_0^\ell \sin \frac{\bar{p}\pi z_2}{\ell} dz_2 \int_0^{2\pi} \cos \bar{n}\phi_1 \, d\phi_1 \int_0^{2\pi} \cos \bar{q}\phi_2 \, d\phi_2 \times$$
$$\left[\int_{-\infty}^{+\infty} h_w(\bar{m},\bar{n},u_1) e^{iwu_1} du_1 \right] \left[\int_{-\infty}^{+\infty} h_w(\bar{p},\bar{q},u_2) e^{-iwu_2} du_2 \right] \times$$
$$\left\{ \left[\int_{-\infty}^{+\infty} \lim_{T\to\infty} \frac{1}{2T} \int_{-T}^{+T} \bar{p}(z_1,\phi_1, t-u_1)\, \bar{p}(z_2,\phi_2, t-u_2+\tau) \, dt \right] e^{-iw\tau_3} d\tau_3 \right\} \qquad [38]$$

Since the process is stationary the correlation function is only a function of $\theta_1 - \theta_2$, or it is only a function of τ_3. This whole term in $\{\ \}$ is the cross spectral density of the loading - denote it by $S_f(z_1,\phi_1,z_2,\phi_2,\omega)$

Then

$$\bar{I}_1 = \frac{4}{\pi^2 \ell^2} \int_0^\ell \sin \frac{\bar{m}\pi z_1}{\ell} dz_1 \int_0^\ell \sin \frac{\bar{p}\pi z_2}{\ell} dz_2 \int_0^{2\pi} \cos \bar{n}\phi_1 \, d\phi_1 \int_0^{2\pi} \cos \bar{q}\phi_2 \, d\phi_2 \times$$
$$\left[H_w(\bar{m},\bar{n},\omega) \right] \left[H_w^*(\bar{p},\bar{q},\omega) \right] \left[S_f(z_1,\phi_1,z_2,\phi_2,\omega) \right] \qquad [39]$$

Thus

$$\int_{-\infty}^{+\infty} \langle v_{\bar{m}\bar{n}}(t)\, v_{\bar{p}\bar{q}}(t+\tau) \rangle e^{-iw\tau} d\tau = H_w(\bar{m},\bar{n},\omega) H_w^*(\bar{p},\bar{q},\omega) C_{v_{\bar{m}\bar{n}} v_{\bar{p}\bar{q}}}$$

$$C_{v_{\bar{m}\bar{n}} v_{\bar{p}\bar{q}}} = \frac{4}{\pi^2 \ell^2} \int_0^\ell \int_0^\ell \int_0^{2\pi} \int_0^{2\pi} S_f(\xi_1,\eta_1,\xi_2,\eta_2,\omega) \sin \frac{\bar{m}\pi\xi_1}{\ell} \sin \frac{\bar{p}\pi\xi_2}{\ell} \cos \bar{n}\eta_1 \cos \bar{q}\eta_2 \, d\xi_1 d\eta_1 d\xi_2 d\eta_2$$

$$\int_{-\infty}^{+\infty} \langle u_{\bar{m}\bar{n}}(t)\, u_{\bar{p}\bar{q}}(t+\tau) \rangle e^{-iw\tau} d\tau = K_w(\bar{m},\bar{n},\omega) K_w^*(\bar{p},\bar{q},\omega) C_{u_{\bar{m}\bar{n}} u_{\bar{p}\bar{q}}}$$

$$C_{u_{\bar{m}\bar{n}} u_{\bar{p}\bar{q}}} = \frac{4}{\pi^2 \ell^2} \int_0^\ell \int_0^\ell \int_0^{2\pi} \int_0^{2\pi} S_f(\xi_1,\eta_1,\xi_2,\eta_2,\omega) \sin \frac{\bar{m}\pi\xi_1}{\ell} \sin \frac{\bar{p}\pi\xi_2}{\ell} \sin \bar{n}\eta_1 \sin \bar{q}\eta_2 \, d\xi_1 d\eta_1 d\xi_2 d\eta_2 \qquad [40]$$

$$\int_{-\infty}^{+\infty} \langle u_{\bar{m}\bar{n}}(t)\, v_{\bar{p}\bar{q}}(t+\tau) \rangle e^{-iw\tau} d\tau = K_w(\bar{m},\bar{n},\omega) H_w^*(\bar{p},\bar{q},\omega) C_{u_{\bar{m}\bar{n}} v_{\bar{p}\bar{q}}}$$

$$C_{u_{\bar{m}\bar{n}} v_{\bar{p}\bar{q}}} = \frac{4}{\pi^2 \ell^2} \int_0^\ell \int_0^\ell \int_0^{2\pi} \int_0^{2\pi} S_f(\xi_1,\eta_1,\xi_2,\eta_2,\omega) \sin \frac{\bar{m}\pi\xi_1}{\ell} \sin \frac{\bar{p}\pi\xi_2}{\ell} \sin \bar{n}\eta_1 \cos \bar{q}\eta_2 \, d\xi_1 d\eta_1 d\xi_2 d\eta_2$$

$$\int_{-\infty}^{+\infty} \langle v_{\bar{m}\bar{n}}(t)\, u_{\bar{p}\bar{q}}(t+\tau) \rangle e^{-iw\tau} d\tau = H_w(\bar{m},\bar{n},\omega) K_w^*(\bar{p},\bar{q},\omega) C_{v_{\bar{m}\bar{n}} u_{\bar{p}\bar{q}}}$$

$$C_{v_{\bar{m}\bar{n}} u_{\bar{p}\bar{q}}} = \frac{4}{\pi^2 \ell^2} \int_0^\ell \int_0^\ell \int_0^{2\pi} \int_0^{2\pi} S_f(\xi_1,\eta_1,\xi_2,\eta_2,\omega) \sin \frac{\bar{m}\pi\xi_1}{\ell} \sin \frac{\bar{p}\pi\xi_2}{\ell} \sin \bar{n}\eta_1 \cos \bar{q}\eta_2 \, d\xi_1 d\eta_1 d\xi_2 d\eta_2$$

The response functions for lateral deflection are equal, i.e.

$$H_w = K_w \qquad [41]$$

(This can be verified by using the basic differential equations for the shell)

Thus, neglecting product terms[*] such as $H_{w}(m,n,\omega)H^{*}_{w}(p,q,\omega)$ we obtain

$$\widetilde{w}(z_{1},\phi_{1},z_{2},\phi_{2},\omega)\approx \frac{1}{2\pi}\sum_{\bar{m}}\sum_{\bar{n}} \sin\frac{\bar{m}\pi z_{1}}{\ell}\sin\frac{\bar{m}\pi z_{2}}{\ell}\,|H_{w}(\bar{m},\bar{n},\omega)|^{2}\times \tag{42}$$

$$[C_{V_{\bar{m}\bar{n}}V_{\bar{m}\bar{n}}}\cos\bar{n}\phi_{1}\cos\bar{n}\phi_{2}$$
$$+C_{U_{\bar{m}\bar{n}}V_{\bar{m}\bar{n}}}\sin\bar{n}(\phi_{1}+\phi_{2})$$
$$+C_{U_{\bar{m}\bar{n}}U_{\bar{m}\bar{n}}}\sin\bar{n}\phi_{1}\sin\bar{n}\phi_{2}]$$

$$\widetilde{a}_{m}(z_{1},\phi_{1},z_{2},\phi_{2},\omega)=\omega^{4}\widetilde{w}(z_{1},\phi_{1},z_{2},\phi_{2},\omega)$$

$\widetilde{a}_{m}$ being the cross spectral density of acceleration.

The solution for the internal pressure field follows directly from the analysis. We just have to remark that for an infinite cylinder each structural mode gives rise to an acoustic mode inside which has a longitudinal and peripheral pressure distribution the same as the shell radial displacement. The auto spectral density of the pressure inside the cylinder at point r, ϕ, z at frequency ω can then be written

$$\widetilde{P}_{i}(r,\phi,z,\omega)\approx\frac{1}{2\pi}\sum_{\bar{m}}\sum_{\bar{n}}\sin^{2}\frac{\bar{m}\pi z}{\ell}\,|H_{p_{i}}(r,\bar{m},\bar{n},\omega)|^{2}\times \tag{43}$$

$$[C_{V_{\bar{m}\bar{n}}V_{\bar{m}\bar{n}}}\cos^{2}\bar{n}\phi$$
$$+2C_{U_{\bar{m}\bar{n}}V_{\bar{m}\bar{n}}}\sin\bar{n}\phi\cos\bar{n}\phi$$
$$+C_{U_{\bar{m}\bar{n}}U_{\bar{m}\bar{n}}}\sin^{2}\bar{n}\phi]$$

where H_{pi} is the frequency response function for internal pressure, i.e. if the pressure on the surface has the form

$$P_{s}(z,\phi,t)=\cos\bar{n}\phi\sin\frac{\bar{m}\pi z}{\ell}e^{i\omega t} \tag{44}$$

then the pressure inside will be determined by the elastic vibration of the wall and the coupling to the air inside and will be given by

$$P_{i}(r,\phi,z,t)=H_{p_{i}}(\bar{m},\bar{n},r,\omega)\cos\bar{n}\phi\sin\frac{\bar{m}\pi z}{\ell}e^{i\omega t} \tag{45}$$

Consider the average internal pressure over cylindrical contours inside the cylinder at various distances r from the center. If we integrate over the area of any of these contours and divide by the area we will obtain[**]

$$[\widetilde{P}_{i}(r,\omega)]_{Ave}\approx\frac{1}{8\pi}\sum_{\bar{m}}\sum_{\bar{n}}|H_{p_{i}}(r,\bar{m},\bar{n},\omega)|^{2}[C_{V_{\bar{m}\bar{n}}V_{\bar{m}\bar{n}}}+C_{U_{\bar{m}\bar{n}}U_{\bar{m}\bar{n}}}] \tag{46}$$

---

[*]Product terms are being neglected in order to reduce the problem to one which is mathematically tractable. In reality product terms are only small if the natural frequencies of the structure are well separated and if the damping is small (i.e. each resonance peak is high). For the time being since we are looking for order of magnitude answers we will neglect them.

[**]This same average would be obtained from [35] even if cross product terms were not neglected.

At this point it is interesting to note that we have considered pressure proportional to $\sin \frac{m\pi x}{\ell}$ which corresponds to an open ended shell, thus

$$(\tilde{P_i})_{Ave} = \text{Average Spectral Density} \sim \int_0^\ell \sin^2 \frac{m\pi z}{\ell} \to \ell \qquad [47]$$

If we had considered a shell with closed ends

$$(\tilde{P_i})_{Ave} \sim \int_0^\ell \cos^2 \frac{m\pi z}{\ell} \to \ell \qquad [48]$$

For one end closed and one open

$$(\tilde{P_i})_{Ave} \sim \int_0^\ell \cos^2 \frac{m\pi z}{2\ell} \to \ell \qquad [49]$$

So that $(\tilde{P_i})_{Ave}$ turns out the same for various practical acoustic boundary conditions which are physically quite different from each other.

B. Calculation of the frequency response function for inside pressure

The Flügge equations of motion for a cylindrical shell can be reduced to a single equation by neglecting longitudinal and tangential inertia. This equation is as follows:[6]

$$D\left\{ \nabla^4 w + \frac{1}{a^4}\nabla^{-4}\left[\frac{12(1-\nu^2)}{(h/a)^2} \frac{\partial^4 w}{\partial z^4} + \frac{2(2-\nu)}{a^2}\frac{\partial^6 w}{\partial z^4 \partial \varphi^2} + \frac{1}{a^4}\frac{\partial^4 w}{\partial \varphi^2} + 2\nu a^2 \frac{\partial^6 w}{\partial z^6} \right.\right.$$
$$\left.\left. + 6\frac{\partial^6 w}{\partial z^4 \partial \varphi^2} + \frac{2(4-\nu)}{a^2}\frac{\partial^6 w}{\partial z^2 \partial \varphi^4} + \frac{2}{a^4}\frac{\partial^6 w}{\partial \varphi^6} \right] \right\} \qquad [50]$$
$$+ \rho h \frac{\partial^2 w}{\partial t^2} = \bar{p}(a,z,\varphi,t) + \bar{p}_{f_i}(a,z,\varphi,t)$$

where $\quad D = E h^3/12(1-\nu^2)$

$\nu = $ Poisson's Ratio

$h = $ cylinder thickness

$\bar{p}(a,z,\varphi,t) = $ external pressure at $r=a$ (forcing pressure)

$\bar{p}_{f_i}(a,z,\varphi,t) = $ internal acoustic pressure at $r=a$ (reaction pressure)

$\nabla^4 = \left(\frac{\partial^2}{\partial z^2} + \frac{1}{a^2}\frac{\partial^2}{\partial \varphi^2} \right)^2 \; ; \; \nabla^{-4} = $ inverse of ∇^4

The fluid pressure on the inside of the shell, $\bar{p}_{f_i}$, is the solution of the wave equation

$$C_i^2 \nabla^2 \bar{p}_{f_i} = \frac{\partial^2 \bar{p}_{f_i}}{\partial t^2} \qquad [51]$$

where C_i is the sound velocity in the air inside the shroud.

The solution for the Fourier component lateral displacement in the mnth mode can be written

$$w_{mn} = C_{mn} \sin \frac{m\pi z}{\ell} \cos n\varphi \, e^{i\omega t} \qquad [52]$$

and the solution for the corresponding pressure inside the shell can be written

$$(\bar{p}_{f_i})_{mn} = P_{mn}(r) \cos n\varphi \sin \frac{m\pi z}{\ell} e^{i\omega t} \qquad [53]$$

-9-

The function pmn(r) can take on two possible values as follows:

$$\text{If} \quad \bar{m}\pi/\ell > \omega/c_i \qquad p_{\bar{m}\bar{n}}(r) = D_{\bar{m}\bar{n}} I_{\bar{n}}(k_r' r) \tag{54}$$

$$\bar{m}\pi/\ell < \omega/c_i \qquad p_{\bar{m}\bar{n}}(r) = D_{\bar{m}\bar{n}} J_{\bar{n}}(k_r r)$$

$$\text{where} \qquad k_r = \sqrt{\frac{\omega^2}{c_i^2} - \frac{\bar{m}^2 \pi^2}{\ell^2}} \tag{55}$$

$$k_r' = \sqrt{\frac{\bar{m}^2 \pi^2}{\ell^2} - \frac{\omega^2}{c_i^2}}$$

The constant Dmn is determined from the boundary condition at the inner surface of the shell

$$w_{\bar{m}\bar{n}}(a, z) = \left(\frac{1}{\rho_i \omega^2} \frac{\partial(p_{f_i})_{\bar{m}\bar{n}}}{\partial r} \right)_{r=a} \tag{56}$$

Thus

$$p_{\bar{m}\bar{n}}(r) = \rho_i \omega^2 C_{\bar{m}\bar{n}} \gamma_{\bar{m}\bar{n}}(r) \tag{57}$$

$$\text{where} \qquad \gamma_{\bar{m}\bar{n}}(r) = \frac{J_{\bar{n}}(k_r r)}{J_{\bar{n}}'(k_r a)} \qquad for \quad \omega/c_i > \bar{m}\pi/\ell$$

$$= \frac{I_{\bar{n}}(k_r r)}{I_{\bar{n}}'(k_r a)} \qquad for \quad \omega/c_i < \bar{m}\pi/\ell$$

In order to determine the frequency response function as indicated in Section III A $\bar{p}(a, z, \phi, t)$ is set equal to the mnth modal component as follows:

$$\bar{p}(a, z, \phi, t) = \cos \bar{n}\theta \sin \frac{\bar{m}\pi z}{\ell} e^{i\omega t} \tag{58}$$

Combining [52], [53], [54], [57] and [58] with [46] the space averaged power spectrum of the inside pressure at r = a can be written as follows:

$$\left[P_i(a, \omega) \right]_{Avg.} = \frac{1}{4} \sum_{\bar{m}} \sum_{\bar{n}} |H_{\bar{m}\bar{n}}|^2 [C_{\bar{m}\bar{n}}] \tag{59}$$

where

$$|H_{\bar{m}\bar{n}}|^2 = \left(\frac{\rho_i}{\rho} \right)^2 \left(\frac{a}{\ell} \right)^2 \left(\frac{\omega}{\omega_{\bar{m}\bar{n}}} \right)^4 \frac{\gamma_{\bar{m}\bar{n}}^2}{|\bar{z}|^2} \tag{60}$$

in which

$$\gamma_{\bar{m}\bar{n}} = \frac{J_{\bar{n}}(k_r a)}{k_r a [-J_{\bar{n}+1}(k_r a) + \frac{\bar{n}}{k_r a} J_{\bar{n}}(k_r a)]} \qquad if \quad \omega/c_i > \bar{m}\pi/\ell \tag{61}$$

$$= \frac{I_{\bar{n}}(k_r' a)}{k_r' a [I_{\bar{n}+1}(k_r' a) + \frac{\bar{n}}{k_r' a} I_{\bar{n}}(k_r' a)]} \qquad if \quad \omega/c_i < \bar{m}\pi/\ell$$

$$|\bar{z}|^2 = \left\{ 1 - \left[\left(\frac{\omega}{\omega_{\bar{m}\bar{n}}} \right)^2 \left(1 + \frac{\rho_i}{\rho} \frac{\gamma_{\bar{m}\bar{n}}}{\frac{\ell}{a} \frac{\omega a}{c_i}} \right) \right] \right\}^2 + \left\{ 2\int \frac{\omega}{\omega_{\bar{m}\bar{n}}} \right\}^2 \tag{62}$$

$$\omega_{\bar{m}\bar{n}} = \frac{C_L}{a} \sqrt{D_9} \; ; \quad where \quad D_9 = P_8(1-\nu^2) + \frac{\ell^2}{12a^2}(D_7 + D_8 D_4)$$

$$D_4 = P_3 - 6\bar{n}^2 - \left[2(4-\nu)\bar{n}^4 / (\frac{\bar{m}\pi a}{\ell})^2 \right] - 2\bar{n}^6 / (\frac{\bar{m}\pi a}{\ell})^4 \tag{62a}$$

$$D_3 = \left[2(2-\nu)\bar{n}^2 / (\frac{\bar{m}\pi a}{\ell})^2 \right] + \bar{n}^4 / (\frac{\bar{m}\pi a}{\ell})^4 - 2\nu (\frac{\bar{m}\pi a}{\ell})^2$$

$$D_8 = (\bar{m}\pi a/\ell)^4 / D_7 \; ; \quad D_7 = \left[(\frac{\bar{m}\pi a}{\ell})^2 + \bar{n}^2 \right]^2$$

For the correlation function given in eq. (20a), (see eq. [46]),[*]

$$C_{m\bar{n}} = [C_{v_{m\bar{n}}v_{m\bar{n}}} + C_{u_{m\bar{n}}u_{m\bar{n}}}]$$ [64]

$$= \frac{4}{\pi^2 \ell^2} \int_0^\ell \int_0^\ell \int_0^{2\pi} \int_0^{2\pi} \frac{\sin k |\xi_1 - \xi_2|}{k|\xi_1 - \xi_2|} \frac{\sin k a|\eta_1 - \eta_2|}{ka|\eta_1 - \eta_2|} \sin \frac{m\pi \xi_1}{\ell} \sin \frac{m\pi \xi_2}{\ell} \cos \bar{n}(\eta_1 - \eta_2) d\xi_1 d\xi_2 d\eta_1 d\eta_2$$

Thus

$$T = \frac{[\tilde{P}_i(a,\omega)]_{Avg.}}{P_0(\omega)} = \frac{1}{8\pi} \sum_m \sum_{\bar{n}} |H_{m\bar{n}}|^2 \frac{C_{m\bar{n}}}{P_0(\omega)}$$ [65]

IV. Response of the unstiffened shroud

A sketch of the unstiffened shroud and inside spacecraft box is shown in Figure 1. The division into grid points is also indicated on the sketch. For purposes of computing the finite element response, the shroud was divided into 80 grid points and the spacecraft box into 60, giving 140 grid points with 420 degrees of freedom (i.e. three displacements at each grid point).

A. Structural path response

Let us focus our attention on the spacecraft box and its attachment to the shroud and compute the response of two corners of the box due to an outside pressure on the shroud and the attachment point to the shroud. In section IIA the RMS displacement (eq. [17]) was found to be

$$\eta_j(RMS) = \left[\sum_m \frac{C_{mm}(\omega_m) z_{jm}^2}{8\beta_m \omega_m^3} \right]^{\frac{1}{2}}$$

It was decided in Section IIB to use a constant value of $C_{mm}(\omega_m)$. It will also be assumed that β_m, the model damping ratio, is also a constant. Taking C_{mm} and β_m outside the summation we can write η_j(RMS) in the following simplified form:

Letting $\quad C_{mm}(\omega_m) = C' P_0(\omega) \ , \ \beta_m = \beta'$

$$\eta_j(RMS) = \left[\frac{C' P_0(\omega)}{8\beta'} \sum_m \frac{z_{jm}^2}{\omega_m^3} \right]^{\frac{1}{2}} = \left[\frac{C' P_0(\omega)}{8\beta'} \right]^{\frac{1}{2}} [T_{s\eta}]^{\frac{1}{2}}$$ [66]

Similarly the RMS acceleration can be written

$$q_j(RMS) = \left[\frac{C' P_0(\omega)}{8\beta'} \sum_m z_{jm}^2 \omega_m \right]^{\frac{1}{2}} = \left[\frac{C' P_0(\omega)}{8\beta'} \right]^{\frac{1}{2}} [T_{sa}]^{\frac{1}{2}}$$ [67]

where $T_{s\eta}$ is the structural path transmission coefficient for displacement and T_{sa} is the structural path transmission coefficient for acceleration. The transmission coefficients $T_{s\eta}$ & T_{sa} have been computed for several third octave bands.

A typical structural transmission path would be from the bottom shroud ring through the truss bar to the bottom of the box and then through the box panels to the top of the box. Therefore representative results can be obtained by tracing the response from a point on the bottom ring

---

[*]See Appendix I for the evaluation of this integral.

(point 79) to a point at the bottom of the box (point 129) and then to a point at the top of the box (point 81).

The results for several third octave bands in the low frequency region are shown in Table 3 together with the contributing modes. Some of these contributing modes are shown in Figures three to eight.

Table 3 Structural Transmission Coefficients for Unstiffened Shroud

1/3 Octave Band Center Freq.-cps	Modes Contributing to The Response	Point on Structure	Component of Displacement or Acceleration	$\frac{Ts_\eta}{10^{-6}}$	$\frac{Tsa}{10^3}$
64	10 - 13	79	r	.55	12.57
			φ	.16	4.86
			z	.008	.18
		129	x	.29	6.48
			η_z	.29	6.58
			z	.01	.22
		81	x	.044	.95
			η_z	.044	.96
			z	.01	.24
160	25 - 31	79	r	.0011	1.16
			φ	.00037	.396
			z	.00061	.49
		129	x	.0011	.82
			η_z	.0011	.81
			z	.00015	.81
		81	x	.0059	7.43
			η_z	.0059	7.51
			z	.00039	.49
640	100-110	79	r	.000098	23.12
			φ	.0000093	2.14
			z	.000073	19.78
		129	x	.000048	8.70
			η_z	.000051	9.18
			z	.000016	3.64
		81	x	.00022	44.85
			η_z	.00023	46.97
			z	.000012	2.44

Referring to relations [66] and [67] and noting that both C' and β' are constants (independent of frequency) Table 3 shows how much greater the displacements are at the low frequencies. Since the acceleration spectrum is essentially ω^4 times the displacement the acceleration at the higher frequencies is in general, greater than at lower frequencies. By tracing the displacement and acceleration transmission functions from point 79 (at the

-12-

bottom ring of the shroud where the truss bar is attached - see Fig. 1) to point 129 (where the truss bar is attached to the spacecraft box) one can see how the motion is amplified or attenuated in structural transmission. One cannot (and should not) determine a pattern as a function of frequency because this will be determined strictly by the character of the structure and its modal content in the frequency band being considered.

B. Acoustic path response

The figure below illustrates the transmission
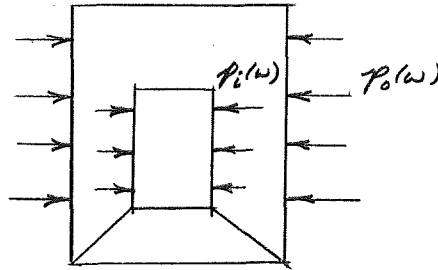
Acoustic Transmission Through the Shroud

of acoustic waves from the outside through the shroud to the spacecraft. Equation [59] gives the average acoustic pressure spectrum at the inside surface of the shroud. The response of the spacecraft box due to the acoustic waves transmitted through the shroud can be written as follows: (see equation [16]), assuming $C_{mm} = \bar{C}'$ = constant,

$$\eta_j (RMS) \approx \left[\frac{\bar{C}' p_i(\omega)}{2\pi} \sum_m Z_{jm}^2 \int_{-\Omega_1}^{\Omega_2} |Y_m(\Omega)|^2 d\Omega \right]^{1/2} \tag{68}$$

$$q_j (RMS) \approx -\Omega_c^2 \eta_j (RMS) \tag{69}$$

$$\Omega_c = \text{center frequency of band}$$

where $\bar{C}' p_i(\omega)$ takes on the parallel role for the box as $c' p_0(\omega)$ does for the shroud. The ratio of the RMS displacements via the structural path and acoustic path can therefore be written as follows:[*]

$$\frac{q_j (RMS)_{struct.}}{q_j (RMS)_{Acoust.}} = \frac{\eta_j (RMS)_{struct.}}{\eta_j (RMS)_{Acoust.}} = \left[\frac{c' p_0(\omega)}{\bar{C}' p_i(\omega)} \right]^{1/2} \tag{70}$$

The c' and $\bar{C}'$ can be written in terms of correlation area as follows: (see equation [22] and [23])

$$c' = \left(\frac{1}{4} \frac{A_c}{A} \frac{A^2}{M} \right)_{Shroud} \quad ; \quad \bar{C}' = \left(\frac{1}{4} \frac{A_c}{A} \frac{A^2}{M} \right)_{Box} \tag{71}$$

---

[*] i.e. the ratio in one frequency band

-13-

It seems reasonable to assume that the ratios of Ac/A are the same if a reverberant field is outside the shroud. Since M is the same for both shroud and box (i.e. it is merely the modal mass which itself does not change radically in the lower modes)

$$\frac{\eta_\partial (RMS)_{struct.}}{\eta_i (RMS)_{Acoust.}} = \frac{A_{shroud}}{A_{Box}} \times \left[\frac{P_o(\omega)}{P_i(\omega)}\right]^{1/2} \qquad [72]$$

where A_{shroud} is the surface area of the shroud and A_{Box} is the surface area of the box.

For the unstiffened shroud

$$\frac{A_{shroud}}{A_{Box}} = 3.61 \qquad [73]$$

The ratio of P_o/P_i is given merely by equation [65] and is the acoustic transmission function.

This acoustic transmission function is given in Table 4 for three frequencies in the low frequency region.

Table 4   Unstiffened Shroud - Acoustic Transmission
Function for the correlation function given in eq. (20a)*

Frequency (cps)	T	Noise Reduction (db)	T (Resonant Modes Alone)	$\frac{(\eta_j)_{struct.}}{(\eta_i)_{Acoust.}}$
64	.17	7.7	.100	8.8
160	.09	10.4	.010	12.0
600	.06	12.1	.007	14.4

By using equation [72], [73] and the values given in the table, it is thus seen that the response due to the acoustic path transmission is only a fraction of that due to the structural path transmission at the three frequencies considered and this would undoubtedly be true at all frequencies in between those considered.

V. Response of the Stiffened Shroud

A. Structural path response

A sketch of the stiffened shroud and inside spacecraft box is shown in Figure 9.[7] The points to focus upon are point 1 (which is the point where the bottom frame is attached to the truss bar, point 121 which is at the bottom of the box, and point 73 at the top of the box.

The results for the structural path for several third octave bands in the low frequency region are shown below in Table 5.

*These are transmission functions at a given frequency and not third octave band values

-14-

Table 5 Structural Transmission Coefficients for Stiffened Shroud

1/3 Octave Band Center Freq.-Cps	Modes Contributing to the Response	Point on Structure	Component of Displacement or Acceleration	$\dfrac{Ts_\eta}{10^{-6}}$	$\dfrac{Tsa}{10^{3}}$
80	1 – 3	1	r	.10	5.54
			φ	.027	1.14
			z	.0000036	.0002
		121	x	.13	6.97
			y	.54	33.1
			z	.0004	.022
		73	x	.04	2.13
			y	.55	33.5
			z	.0006	.033
100	4 – 6	1	r	.00026	.05
			φ	.0056	1.04
			z	.00072	.14
		121	x	.11	20.2
			y	.4	62.1
			z	.0002	.04
		73	x	.092	17.2
			y	.38	58.6
			z	.00006	.01
160	12 – 14	1	r	.0017	1.95
			φ	.0055	4.33
			z	.0001	.12
		121	x	.0059	6.9
			y	.0004	.057
			z	.0054	6.29
		73	x	.25	291
			y	.00004	.0004
			z	.0086	10
222	18 – 24	1	r	.0021	14.2
			φ	.000018	.077
			z	.00012	.812
		121	x	.019	149
			y	.000004	.023
			z	.001	7.7
		73	x	.0014	10.6
			y	.0002	1.1
			z	.0011	8.4
640	73 – 85	1	r	.001	243
			φ	.00015	42
			z	.0003	58.9
		121	x	.000002	.534
			y	.000002	.539
			z	.0000015	3.84
		73	x	.000015	2.75
			y	.000028	6.5
			z	.000034	8.1

B. Acoustic Path Response

The acoustic transmission function is given for the same center frequencies in Table 6.

<center>Table 6   Stiffened Shroud</center>

<center>Acoustic Transmission Function for the correlation function given in eq. (20a)</center>

Frequency (cps)	T	Noise Reduction (db) Theor.	Exper.[7]	T (Resonant modes alone)	$\dfrac{(\eta_j)_{struct.}}{(\eta_j)_{Acoust.}}$
80	.000057	42	–	0	560
100	.000120	39	–	0	390
160	.006700	21	–	.005400	48
222	.003600	24	–	.002900	65
640	.001800	27	21	.000870	93
1200	.005600	22	20	.000280	52
2400	.000550	32	33	.000011	170

Comparing the ratios of structural to acoustic path response of the stiffened to the unstiffened shroud one can see the order of the stiffener effect. The effect is not in the structural path response since this is the same order of magnitude for both stiffened and unstiffened shroud. The greater effect comes about through the acoustic transmission function which is seen to be about an order of magnitude smaller for the stiffened shroud than it is for the unstiffened shroud.

<center>REFERENCES</center>

1. J. E. Greenspon, "Prediction of the Dynamic Environment of Spacecraft Components, Part I. General Concepts and Description of Computer Programs," J G Engineering Research Associates, Contract NAS 5-9124, Tech Rep. No. 5, Dec., 1965.

2. W. C. Hurty and M. F. Rubenstein, "Dynamics of Structures," Prentice Hall, Inc., 1964, p. 395, 405.

3. A. Powell, Jour. Acoust. Soc. Am., 36, 4, 783-784, (1964).

4. D. J. Bozich, Jour. Acoust. Soc. Am., 36, 1, 54-55 (1964).

5. J. V. Rattayya and M. C. Junger, Jour. Acoust. Soc. Am., 36,5, 878-884 (1964).

6. R. W. Leonard and J. M. Hedgepeth, "On Panel Flutter and Divergence of Infinitely Long Unstiffened and Ring Stiffened Thin-Walled Circular Cylinders," NACA Report 1302, 1957.

7. J. E. Manning and N. Koronaios, "Experimental Study of Sound and Vibration Transmission to a Shroud-Enclosed Spacecraft," Bolt, Beranek and Newman, Inc., Contract No. NAS J-10302, 1 August 1968.

---

* In these calculations it was assumed that there was a nodal point at each rib on the shroud (See Fig. 9)

<center>-16-</center>

The model that was built and tested was the stiffened shroud model. The test results are contained in a previously cited report.[7] In Table 6 the experimental values for noise reduction are compared with the theory presented in this report (see Section III and Appendix I). There is good agreement between the theory and experiment for the two highest frequencies in Table 6 (i.e. 1200 and 2400 Hz). Unfortunately there are no experimental results in the lower frequency region (below 300 Hz).

The results of this report show that the structural path dominates the acoustic path at all of the low frequencies (i.e. below 2 Kc) This seems to be at variance with the experimental results since they show that the acoustic path dominates the structural path below 2 Kc. The writer offers a partial explanation for this discrepancy below, but it is difficult to understand how the acoustic path can dominate the structural path when the noise reduction through the shroud is of the order of 20 db if the same coupled shroud-spacecraft modes are involved in the response due to both paths at a given frequency.

In the calculation of the ratio of the response due to the structural and acoustic paths, it was assumed that at a given frequency the entire structure (shroud plus box) responded in the same coupled modes for both paths. As stated above this assumption led to the answer that the structural path was predominant throughout the frequency range considered. It is apparent from the experimental data[7] that in this particular structure this assumption is incorrect and that the box responded independently and with a different set of modes than the coupled shroud-box combination. The fact that the acoustic response of the box alone (when the truss bars were cut) accounts for the difference between the structural path response and the combined response (structural plus acoustic path with the bars connected) seems to support this view.

Appendix I

Computation of the Joint Acceptance $C_{\bar{m}\bar{n}}$

In Section III, eq. [64] gave the following integral:

$$C_{\bar{m}\bar{n}} = \frac{4}{\pi^2 \ell^2} \int_0^\ell \int_0^\ell \int_0^{2\pi} \int_0^{2\pi} \frac{\sin k|\xi_1 - \xi_2|}{k|\xi_1 - \xi_2|} \frac{\sin ka|\eta_1 - \eta_2|}{ka|\eta_1 - \eta_2|} \sin \frac{\bar{m}\pi\xi_1}{\ell} \sin \frac{\bar{m}\pi\xi_2}{\ell} \cos \bar{n}(\eta_1 - \eta_2) \, d\xi_1 d\xi_2 d\eta_1 d\eta_2 \quad \text{[I-1]}$$

letting
$$\xi = \xi_1 - \xi_2 \,, \quad \eta = \eta_1 - \eta_2$$
$$\frac{\xi}{\ell} = x \,, \quad \frac{\xi_1}{\ell} = x_1 \,, \quad \frac{\xi_2}{\ell} = x_2$$
$$\frac{\eta}{\pi} = \theta \,, \quad \frac{\eta_1}{\pi} = \theta_1 \,, \quad \frac{\eta_2}{\pi} = \theta_2$$
$$\quad \text{[I-2]}$$

Thus

$$C_{\bar{m}\bar{n}} = \frac{4}{\pi^2 \ell^2} \times 4\pi^2 \ell^2 \int_0^1 \int_0^1 \int_0^1 \int_0^1 \frac{\sin k\ell x}{k\ell x} \frac{\sin \pi ka\theta}{\pi ka\theta} \sin \bar{m}\pi x_1 \sin \bar{m}\pi x_2 \cos \pi\bar{n}\theta \, dx_1 dx_2 d\theta_1 d\theta_2 \quad \text{[I-3]}$$

Using the results of Powell[3] and White[*]

$$C_{\bar{m}\bar{n}} = 16 \left\{ \frac{1}{2k\ell} \int_0^{k\ell + \bar{m}\pi} \frac{\sin x}{x} dx + \frac{1}{2k\ell} \int_0^{|k\ell - \bar{m}\pi|} \frac{\sin x}{x} dx + \frac{1}{2k\ell}\left[\frac{\cos(k\ell - \bar{m}\pi) - 1}{k\ell - \bar{m}\pi} + \frac{\cos(k\ell + \bar{m}\pi) - 1}{k\ell + \bar{m}\pi} \right] \right.$$
$$\left. - \frac{1}{2\bar{m}\pi k\ell} \left[\int_0^{k\ell + \bar{m}\pi} \frac{\cos x - 1}{x} dx + \left\{ \begin{array}{l} -\int_0^{k\ell - \bar{m}\pi} \frac{\cos x - 1}{x} dx \,, \text{ if } k\ell > \bar{m}\pi \\ +\int_0^{\bar{m}\pi - k\ell} \frac{\cos x - 1}{x} dx \,, \text{ if } k\ell < \bar{m}\pi \end{array} \right] \right\} \quad \text{[I-4]}$$
$$\times \left\{ \frac{1}{\pi ka} \left[\int_0^{\pi(ka + \bar{n})} \frac{\sin x}{x} dx + \int_0^{|\pi(ka - \bar{n})|} \frac{\sin x}{x} dx \right] + \frac{2}{\pi ka} \left[\frac{\cos \pi(ka - \bar{n}) - 1}{\pi(ka - \bar{n})} + \frac{\cos \pi(ka + \bar{n}) - 1}{\pi(ka + \bar{n})} \right] \right\} \right\}$$

The integrals are standard cosine and sine integrals, for which
approximations are given in the literature[**].

[*]P. White, Jour. Acoust. Soc. Am. ,36,4,784-785,(1964).
[**] M. Abramowitz and I. A. Stegun, "Handbook of Mathematical Functions", National Bureau of Standards, 1964,p.233.

Appendix II

Listing of Computer Programs

A. Program for C_{mm} in BASIC Language

The first listing is for the C_{mm} program used to calculate the values in Table 1. Statements 20,40,45,48,70,75,78 of the program are the input values as follows:

M = N = Total number of grid points on the shroud

K = ω/c where ω = radian frequency
c = sound velocity in the air

A = radius of the shroud

Q(I) = mode shape values for grid points 1 to M (these values are given in statements 180-198)

T(I) = angular coordinates of the peripheral grid points (these values are given in statements 200-220)

X(I) = longitudinal coordinates of the grid points (these values are given in statements 240-258)

R(J) = mode shape values for grid points 1 to N (these values are given in statements 300-318)

U(J) }
Z(J) } statements 320-358 are a repetition of 200-258

The output consists of G1, which is C_{mm} .

B. Program for $T_{s\eta}$ and T_{sa} in FORTRAN

In this program the following parameters are inputs:

I1 = subscript of first grid point at which displacement and acceleration are being computed.

I2 = subscript of last grid point at which displacement and acceleration are being computed.

I3 = increment in the I subscript

M1 = subscript of the first mode to be considered in the deflection and acceleration summation.

M2 = subscript of the last mode to be considered in the deflection and acceleration summation.

M3 = increment in the M subscript.

H(M) = natural frequency of the Mth mode (radian)

P(M,I) = mode shape value of Mth mode at Ith point

The output parameters are: DISU = $T_{s\eta}$,ACCU = T_{sa}

In this program the H and P arrays are given in the files as shown below the main program.   -19-

C. Program for Noise Reduction Calculation in BASIC Language

The input parameters are given in statements 5 and 10 and are as follows: (the parameters in statement 11 are dummy parameters always held constant and equal to the values shown in 238)

C5 = ratio of damping to critical damping

C2 = h/a, a = radius of shell
$\qquad$ h = thickness of shell

$C1 = c_L/c_i$, $c_L = \sqrt{\dfrac{E}{\rho(1-\nu^2)}}$
$\qquad$ E = modulus of elasticity of shell
$\qquad\quad$ = Poisson's ratio
$\qquad$ C_i = sound velocity in air inside shell

C4 = a/1 a = shell radius
$\qquad\quad$ 1 = shell length

P1 = m_{min} $\left.\rule{0pt}{2.5em}\right\}$
P2 = m_{max} $\qquad$ m = number of longitudinal half waves in vibration
P3 = m $\qquad\qquad$ pattern

D = $\qquad$ (Poisson's ratio

Q = n_{max} $\qquad$ n = number of circumferential waves in vibration
$\qquad\qquad\qquad$ pattern

T1 = 1.57 $\left.\rule{0pt}{2em}\right\}$ constant for all cases
T2 = 1.57

R1 = ρ_i/ρ $\qquad$ ρ_i = density of air inside shell
$\qquad\qquad$ ρ = density of shell material

H1 = 1/C2

K5 = $\left(\dfrac{\omega a}{c_i}\right)_{min}$

K6 = $\left(\dfrac{\omega a}{c_i}\right)_{max}$

K7 = $\Delta\left(\dfrac{\omega a}{c_i}\right)$ $\qquad\qquad$ ω = frequency

The output parameters are:

C3 = $\dfrac{\omega a}{c_i}$ $\quad$ (printed out for information - it is an input parameter)

T = p_i/p_o $\quad$ transmission function

T5 = noise reduction in db

T8 = p_i/p_o for resonance modes alone

T9 = T8 expressed in db

Program for C$_{mm}$

```
10 DIM Q(30),R(30),T(30),U(30),X(30),Z(80)
20 READ M,N,K,A
30 FOR I= 1 TO M
40 READ Q(I)
45 READ T(I)
48 READ X(I)
50 NEXT I
60 FOR J= 1 TO N
70 READ R(J)
75 READ U(J)
78 READ Z(J)
80 NEXT J
85 LET G1=0
90 FOR J= 1 TO N
100 FOR I= 1 TO M
110 LET G=SIN(X*A*ABS(U(J)-T(I)+.0001))/(K*A*ABS(U(J)-T(I)+.0001))
120 LET H=SIN(K*ABS(Z(J)-X(I)+.0001))/(K*ABS(Z(J)-X(I)+.0001))
130 LET G1 =G1+Q(I)*R(J)*G*H*114.8
140 NEXT I
150 NEXT J
160 PRINT "G1=";G1
170 DATA 30,30,.0303,13
180 DATA -3.506,-2.458,.0187,2.469,3.523,2.504,.0361,-2.45
182 DATA -3.507,-2.492,-.0142,2.463,3.491,2.443,-.0413,-2.503
184 DATA -1.094,-.171,.0012,.173,1.109,.19,.0112,-.136
186 DATA -1.105,-.201,-.0067,.197,1.031,.139,-.0377,-.156
188 DATA 1.660,1.345,-.0145,-1.359,-1.645,-1.35,-.0059,1.386
190 DATA 1.644,1.325,.0018,-1.315,-1.663,-1.33,-.021,1.397
192 DATA 4.615,3.485,-.0268,-3.516,-4.601,-3.51,-.0151,3.513
194 DATA 4.593,3.484,.0102,-3.467,-4.608,-3.506,.0091,3.541
196 DATA 6.866,4.752,-.0307,-4.794,-6.871,-4.789,-.024,4.753
198 DATA 6.856,4.733,.0145,-4.763,-6.81,-4.75,.0397,4.808
200 DATA .0001,.393,.786,1.179,1.572,1.965,2.358,2.751
202 DATA 3.144,3.537,3.93,4.323,4.716,5.109,5.502,5.895
206 DATA .0001,.393,.786,1.179,1.572,1.965,2.358,2.751,3.144
208 DATA 3.537,3.930,4.323,4.716,5.109,5.502,5.895
210 DATA .0001,.393,.786,1.179,1.572,1.965,2.358,2.751,3.144
212 DATA 3.537,3.930,4.323,4.716,5.109,5.502,5.895,6.288
214 DATA .0001,.393,.786,1.179,1.572,1.965,2.358,2.751,3.144
216 DATA 3.537,3.930,4.323,4.716,5.109,5.502,5.895,6.288
218 DATA .0001,.393,.786,1.179,1.572,1.965,2.358,2.751,3.144
220 DATA 3.537,3.930,4.323,4.716,5.109,5.502,5.895,6.288
240 DATA .0001,.0001,.0001,.0001,.0001,.0001,.0001,.0001
242 DATA .0001,.0001,.0001,.0001,.0001,.0001,.0001,.0001
244 DATA 16.25,16.25,16.25,16.25,16.25,16.25,16.25,16.25
246 DATA 16.25,16.25,16.25,16.25,16.25,16.25,16.25,16.25
248 DATA 32.5,32.5,32.5,32.5,32.5,32.5,32.5,32.5
250 DATA 32.5,32.5,32.5,32.5,32.5,32.5,32.5,32.5
252 DATA 48.75,48.75,48.75,48.75,48.75,48.75,48.75,48.75
254 DATA 48.75,48.75,48.75,48.75,48.75,48.75,48.75,48.75
256 DATA 65,65,65,65,65,65,65,65
258 DATA 65,65,65,65,65,65,65,65
```

```
300 DATA -3.506,-2.453,.0187,2.469,3.523,2.504,.0361,-2.45
302 DATA -3.507,-2.492,-.0142,2.468,3.491,2.443,-.0413,-2.503
304 DATA -1.094,-.171,.0012,.178,1.109,.19,.0112,-.136
306 DATA -1.105,-.201,-.0067,.197,1.081,.139,-.0377,-.156
308 DATA 1.660,1.845,-.0145,-1.859,-1.645,-1.85,-.0059,1.886
310 DATA 1.644,1.825,.0018,-1.815,-1.668,-1.83,-.021,1.897
312 DATA 4.615,3.485,-.0262,-3.516,-4.601,-3.51,-.0151,3.513
314 DATA 4.593,3.484,.0102,-3.467,-4.608,-3.506,.0091,3.541
316 DATA 6.866,4.752,-.0307,-4.794,-6.871,-4.739,-.024,4.753
318 DATA 6.856,4.783,.0145,-4.763,-6.85,-4.75,.0397,4.808
320 DATA .0001,.393,.786,1.179,1.572,1.965,2.358,2.751
322 DATA 3.144,3.537,3.93,4.323,4.716,5.109,5.502,5.895
324 DATA .0001,.393,.786,1.179,1.572,1.965,2.358,2.751,3.144
326 DATA 3.537,3.930,4.323,4.716,5.109,5.502,5.895
328 DATA .0001,.393,.786,1.179,1.572,1.965,2.358,2.751,3.144
330 DATA 3.537,3.930,4.323,4.716,5.109,5.502,5.895,6.288
332 DATA .0001,.393,.786,1.179,1.572,1.965,2.358,2.751,3.144
334 DATA 3.537,3.930,4.323,4.716,5.109,5.502,5.895,6.288
336 DATA .0001,.393,.786,1.179,1.572,1.965,2.358,2.751,3.144
338 DATA 3.537,3.930,4.323,4.716,5.109,5.502,5.895,6.288
340 DATA .0001,.0001,.0001,.0001,.0001,.0001,.0001,.0001
342 DATA .0001,.0001,.0001,.0001,.0001,.0001,.0001,.0001
344 DATA 16.25,16.25,16.25,16.25,16.25,16.25,16.25,16.25
346 DATA 16.25,16.25,16.25,16.25,16.25,16.25,16.25,16.25
348 DATA 32.5,32.5,32.5,32.5,32.5,32.5,32.5,32.5
350 DATA 32.5,32.5,32.5,32.5,32.5,32.5,32.5,32.5
352 DATA 48.75,48.75,48.75,48.75,48.75,48.75,48.75,48.75
354 DATA 48.75,48.75,48.75,48.75,48.75,48.75,48.75,48.75
356 DATA 65,65,65,65,65,65,65,65
358 DATA 65,65,65,65,65,65,65,65
600 END
```

Output

$$G1 = 2.24563E+7 = C_{mm}$$

```
10 DIMENSION H(13),P(13,9)
20 DATA I1,I2,I3,M1,M2,M3/1,9,1,1,13,1/
25 CALL OPEN(4,'FILED','INPUT')
28 CALL OPEN(2,'FILEB','INPUT')
30 DO 14 M=M1,M2,M3
50 READ(2)H(M)
60 14 CONTINUE
70 DO 21 I=I1,I2,I3
80 DO 21 M=M1,M2,M3
90 READ (4) P(M,I)
100 21 CONTINUE
110 DISU=0
120 ACCU=0
130 DO 35 I=I1,I2,I3
140 DO 23 M=M1,M2,M3
150 GM=P(M,I)^2
160 DISU=DISU+(GM/(H(M)^3))
170 ACCU=ACCU+(GM*H(M))
180 23 CONTINUE
210 WRITE (6,*)I,DISU,ACCU
212 DISU=0
214 ACCU=0
250 35 CONTINUE
260 CALL CLOSE(1,4)
270 END
```

```
10 DIMENSION P(13,9)
40 DATA P/.0403,-1.166,-.078,5.035,-.012,.0017,3.669,-2.883,%
50 -2.653,.0829,-1.714,.304,-1.395,-.671,.158,.0676,-.0177,.0075,%
60 .738,.0194,-.324,.251,2.469,.0948,1.654,.374,-.256,-2.91,%
70 -.144,2.373,-.0046,.0066,-.65,.485,.949,.384,.0266,.066,.103,%
80 .0044,-.05,-.002,.0376,.135,-.0004,.3,-.0353,.0231,.0071,.122,%
90 -.0033,.0178,-.0562,.0329,-.0094,.0327,.216,-.0525,-.082,-.0535,%
100 .0034,-.0703,.0729,-.132,-.193,-.0039,.0143,-.0019,-.0574,-.0004,%
110 .0003,.502,-.566,-.593,.0046,-.0371,-.0471,.136,-.104,-.76,%
120 -.0346,-.13,.217,.0007,.177,.0696,.033,.089,.0412,-.0298,.2,%
125 -.769,.316,-.0091,.071,.27,-.0714,.366,.0233,.524,-.083,.294,%
130 -.161,-.591,.0421,.436,.0174,-.162,-.0398,-.0005,.732,-.774,%
135 -.841,-.054,-.0026,-.034,.0241/
160 CALL OPEN(4,'FILED','OUTPUT')
170 WRITE(4)P
180 CALL CLOSE (4)
190 END
```

```
10 DIMENSION H(13)
20 DATA H/3592.0,3603.0,3717.0,3757.0,3805.0,3906.0,3923.0,%
30 3959.0,3979.0,4061.0,4377.0,4412.0,4423.0/
160 CALL OPEN(2,'FILEE','OUTPUT')
170 WRITE(2)H
180 CALL CLOSE(2)
190 END
```

23

Output

I	T_{sm}	T_{sa}
1	0.105407E-08	243179.
2	0.146781E-09	42004.4
3	0.316931E-09	58913.6
4	0.223211E-11	534.63
5	0.195716E-11	539.243
6	0.154279E-10	3838.21
7	0.150616E-10	2747.93
8	0.284583E-10	6486.22
9	0.344523E-10	8104.61

```
2 DIM C(100,20),G(100,20),F(100,20)
3 DIM T(50),J(50)
5 READ C5,C2,C1,C4,P1,P2,P3,D,Q
10 READ T1,T2,R1,H1,K5,K6,K7
11 READ L9,Y
12 FOR C3=K5 TO K6 STEP K7
39 FOR P=P1 TO P2 STEP P3
42 LET C6=P*3.1416*C4
45 IF C3<C6 THEN 51
48 IF C3>C6 THEN 66
51 LET Z=SQR((C6^2)-(C3^2))
54 FOR I=0 TO Q
57 LET G(P,I)=1/SQR((I^2)+(Z^2))
60 NEXT I
63 GO TO 90
66 LET Z=SQR((C3^2)-(C6^2))
69 GOSUB 516
72 FOR I=0 TO Q
75 IF I>Z THEN 84
78 LET G(P,I)=1/((-Z*J(I+1)/J(I))+I)
81 GO TO 87
84 LET G(P,I)=1/SQR((I^2)-(Z^2))
87 NEXT I
90 NEXT P
104 FOR P=P1 TO P2 STEP P3
106 LET C6=P*3.1416*C4
108 FOR I=0 TO Q
110 LET D7= ((C6^2) + (I^2))^2
115 LET D8 = (C6^4)/D7
116 LET D3=(2*(2-D)*(I^2)/(C6^2))+(I^4)/(C6^4)-2*D*(C6^2)
118 LET D4=D3-6*(I^2)-(2*(4-D)*(I^4)/(C6^2))-2*(I^6)/(C6^4)
120 LET D9=D8*(1-D^2)+.08333*(C2^2)*(D7+D8*D4)
130 LET R0=C1*SQR(D9)
140 E2=1-((C3/R0)^2)*(1+(R1*G(P,I)/(C3*C2)))
141 IF AES(E2)>2*C5 THEN 145
143 PRINT"RES";"I=";I;"P=";P
144 LET E7=1/((E2^2)+((C3/R0)*2*C5)^2)
145 LET E3=(C3/R0)*2*C5
148 LET A9= (E2^2)+(E3^2)
149 LET A1=C3/C4
151 LET A2=P*3.1416
153 LET X=A1+A2
155 GOSUB 600
157 LET U1=(.5/A1)*(S9+(COS(X)/X)-(1/A2)*C9)
159 IF A1<A2 THEN 167
161 LET X=A1-A2
163 GOSUB 600
165 U2=(.5/A1)*(S9+(COS(X)/X)+(1/A2)*C9)
```

```
166 GO TO 173
167 LET X=A2-A1
169 GOSUB 600
171 U2=(.5/A1)*(S9+(COS(X)/X)-(1/A2)*C9)
173 LET J8=U1+U2
175 X=3.1416*(C3+I)
177 GOSUB 600
179 LET V1=S9+2*(COS(X)-1)/X
181 X=3.1416*ABS(C3-I)
183 GOSUB 600
185 LET V2=S9+2*(COS(X)-1)/X
187 J9=(1/(3.1416*C3))*(V1+V2)
198 B9=J8*J9
200 F(P,I)=((C3/R0)^4)*B9*E7*(R1^2)*(H1^2)
205 C(P,I)=((C3/R0)^4)*B9*(1/A9)*(R1^2)*(H1^2)
208 E7=0
210 IF (R1*G(P,I)/(C3*C2))<.5 THEN 217
214 PRINT "CAV-RES";"I=";I;"P=";P
217 NEXT I
220 NEXT P
223 FOR P=P1 TO P2 STEP P3
224 FOR I=0 TO Q
225 LET T=T+.64*C(P,I)*(G(P,I)^2)
226 LET T8=T8+.64*F(P,I)*(G(P,I)^2)
227 NEXT I
228 NEXT P
229 LET T5=10*LOG(T)/(LOG(10))
230 LET T9=10*LOG(T8)/(LOG(10))
231 PRINT "C3=";C3;"T=";T;"T5=";T5;"T8=";T8;"T9=";T9
232 LET T=0
233 LET T8=0
234 NEXT C3
235 STOP
236 DATA .05,.00544,10,.2,4,80,4,.3,20
237 DATA 1.57,1.57,.000684,184,5.25,6,7
238 DATA 0,.0054
239 LET L(M)=0
240 LET L(M-1)=10^(-L9)
250 FOR I=M TO 2 STEP -1
260 LET L(I-2)=2*(I-1)*(1/Z)*L(I-1) +L(I)
270 NEXT I
275 LET S3=0
280 FOR I=1 TO M
290 LET S3=S3+2*L(I)
300 NEXT I
310 LET S4=EXP(-Z)*(S3+L(0))
320 FOR I=0 TO M
340 LET H(I)=(L(I))/S4
360 NEXT I
370 RETURN
```

```
516 LET M=2*INT(Z)
517 IF M>2 THEN 519
518 LET M=2
519 LET T(M)=0
520 LET T(M-1)=10^(-L9)
521 FOR I=M TO 2 STEP -1
522 LET T(I-2)=2*(I-1)*(1/Z)*T(I-1) - T(I)
524 NEXT I
525 LET S=0
526 FOR I=1 TO M/2
528 LET S=S+2*T(2*I)
530 NEXT I
532 LET S1=S+T(0)
534 FOR I=0 TO M
536 LET J(I)=(T(I))/S1
540 NEXT I
542 RETURN
600 J1=(X^4)+7.241163*(X^2)+2.463936
605 J2=(X^4)+9.06858*(X^2)+7.157433
610 F5=J1/(X*J2)
615 J3=(X^4)+7.547478*(X^2)+1.564072
620 J4=(X^4)+15.723606*(X^2)+12.723684
625 G5=J3/((X^2)*J4)
630 S9=1.5708-F5*COS(X)-G5*SIN(X)
635 C7=F5*SIN(X)-G5*COS(X)
640 C9=C7-LOG(X)-.5772157
645 RETURN
650 END
```

Output

```
RESI= 13  P= 4  ⎫
RESI= 13  P= 8  ⎪
RESI= 7   P= 12 ⎬  Modes which are resonant within the
RESI= 16  P= 12 ⎪  half power points at C3= 5.25
RESI= 12  P= 16 ⎪
RESI= 13  P= 16 ⎭
C3= 5.25  T= 1.61701E-3  F5=-27.9129  F8= 2.54677E-4  T9=-35.9401
```

Fig. 1 Unstiffened Shroud

Grid Points

Cylinder		Box	
1-16	top	81-92	Top Box
17-32	Level 1	93-104	Level A
33-48	Level 2	105-116	Level B
49-64	Level 3	117-128	Level C
65-80	Bottom	129-140	Bottom Box
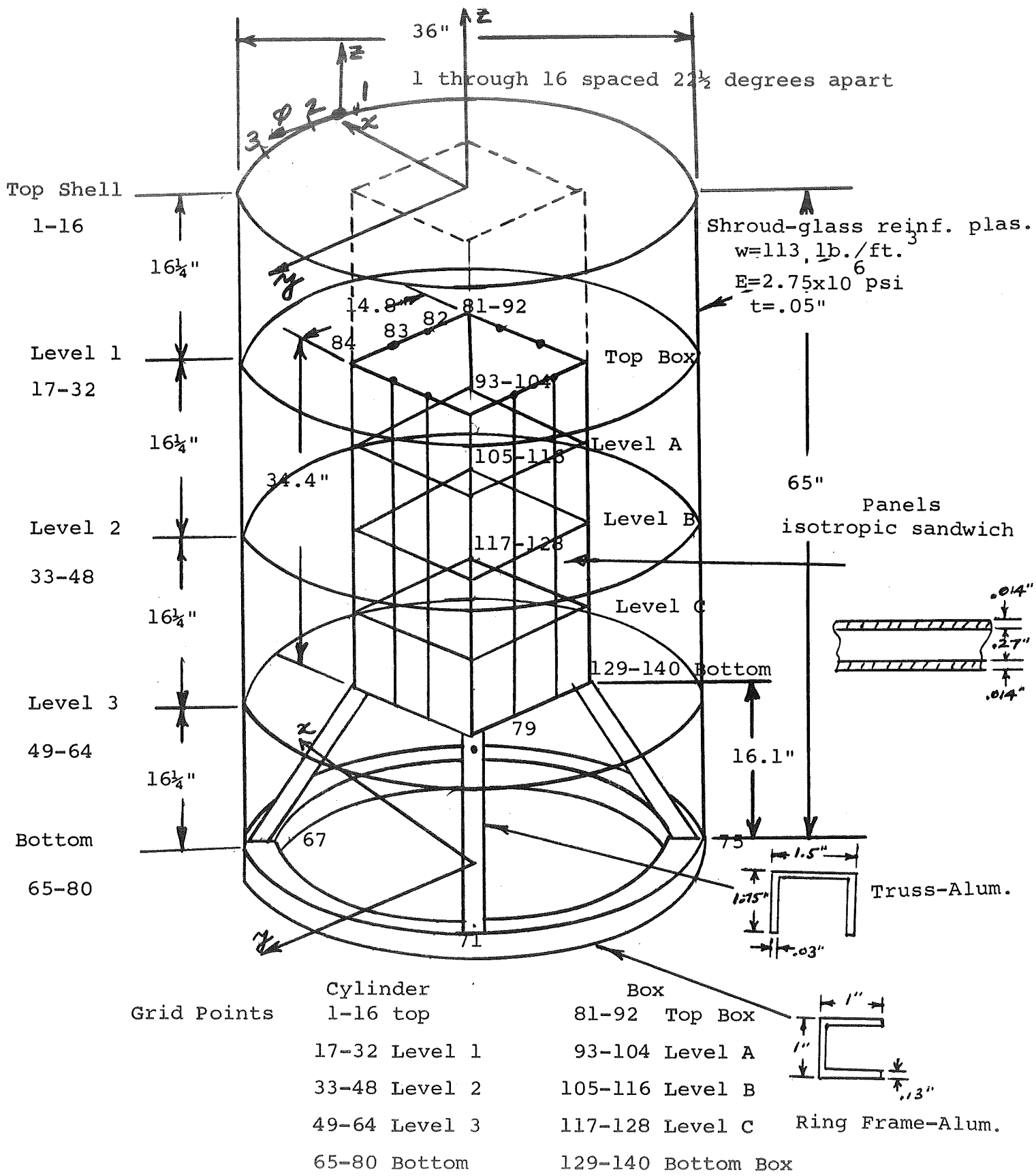
Truss is connected between 67-132, 71-135, 75-138, 79-129

28
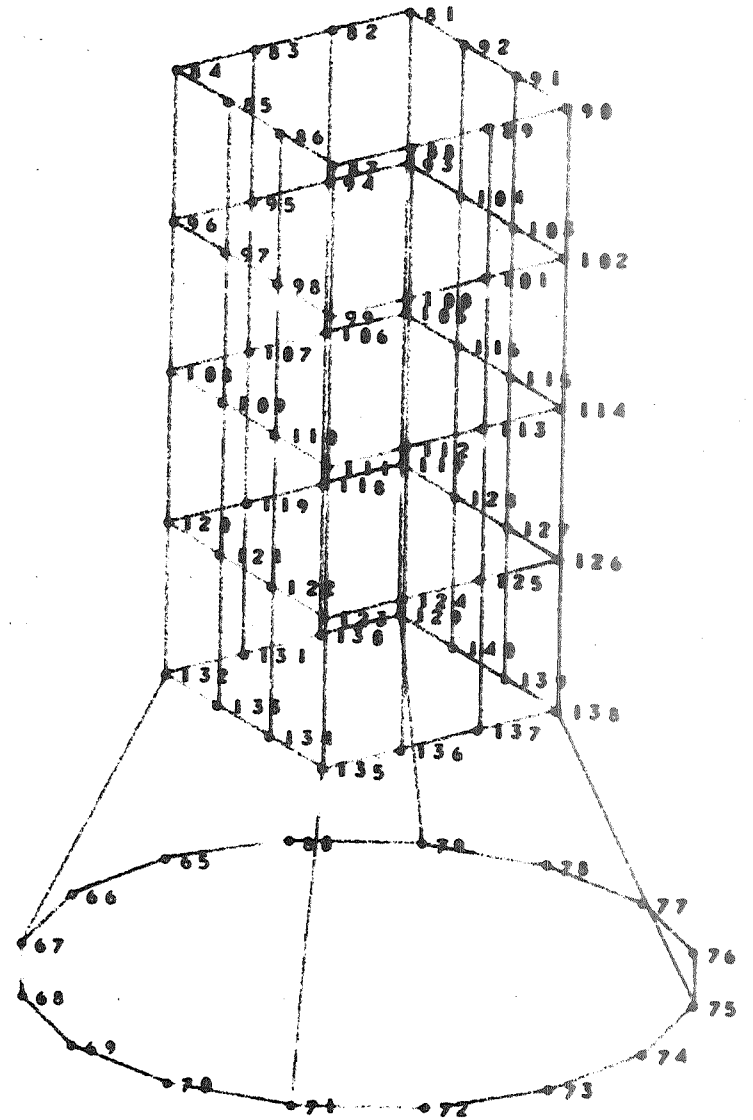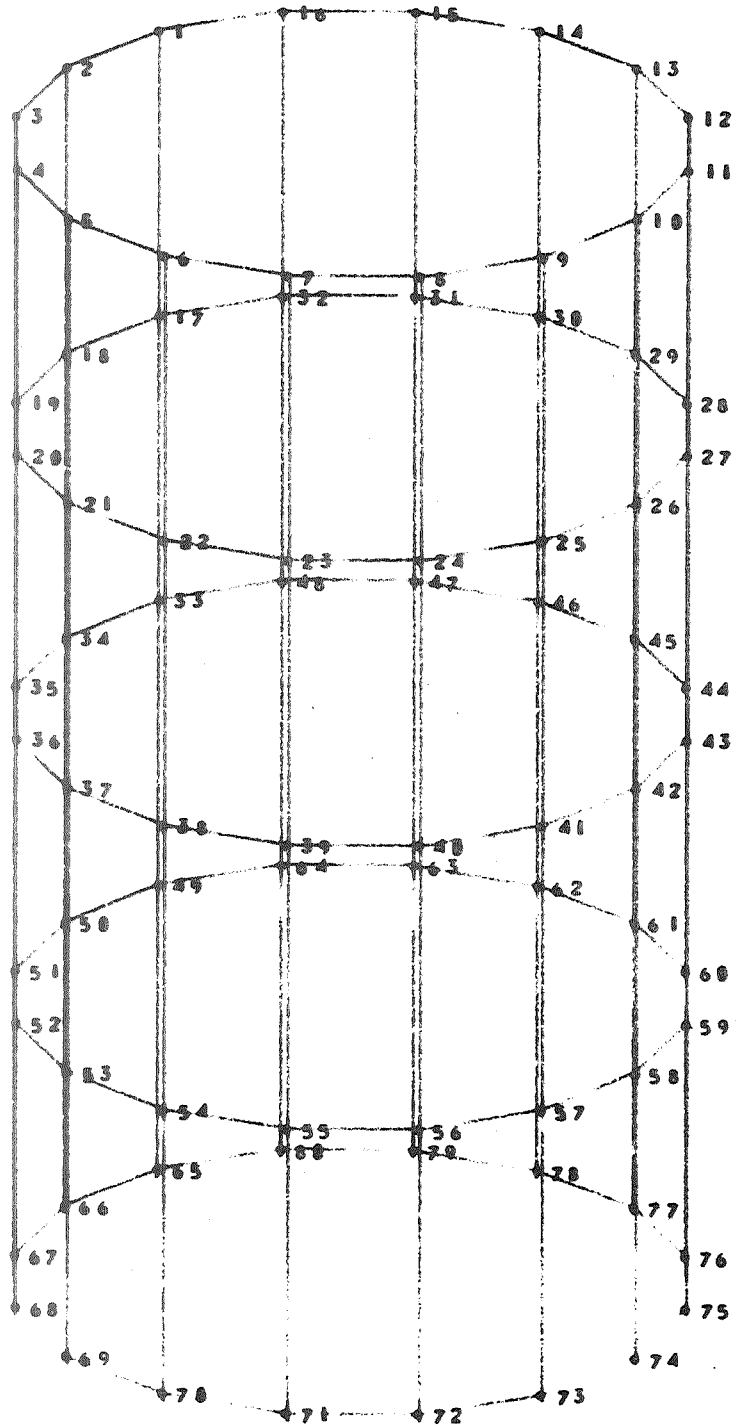
Fig. 2 Grid Points-Unstiffened
Shroud
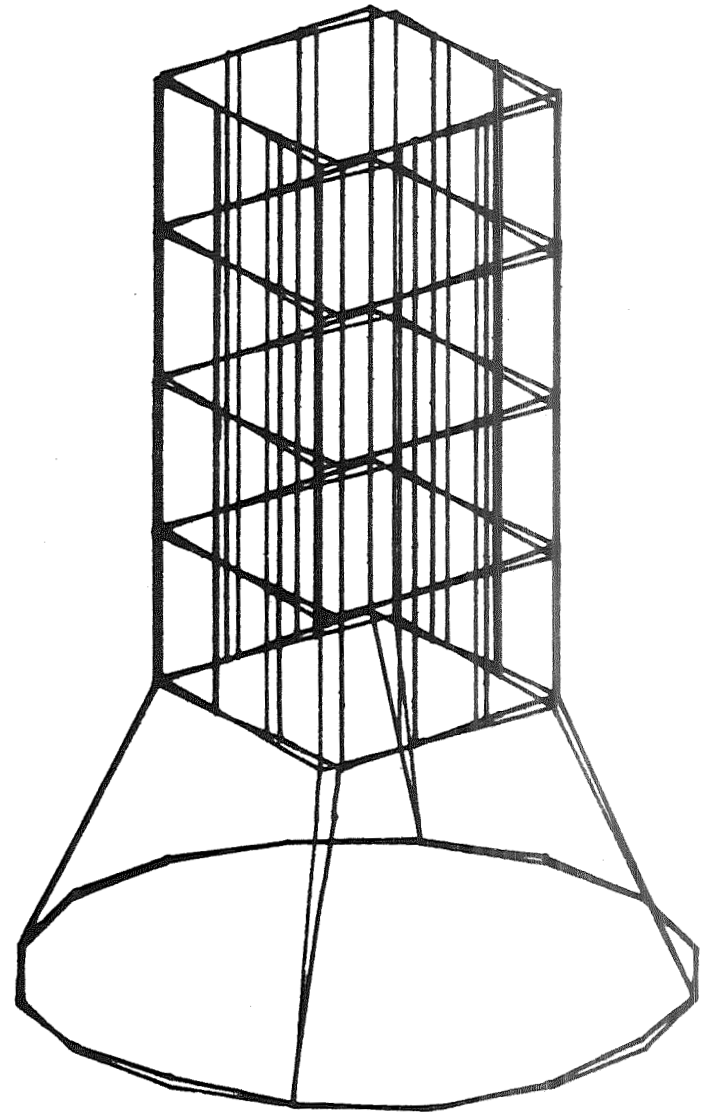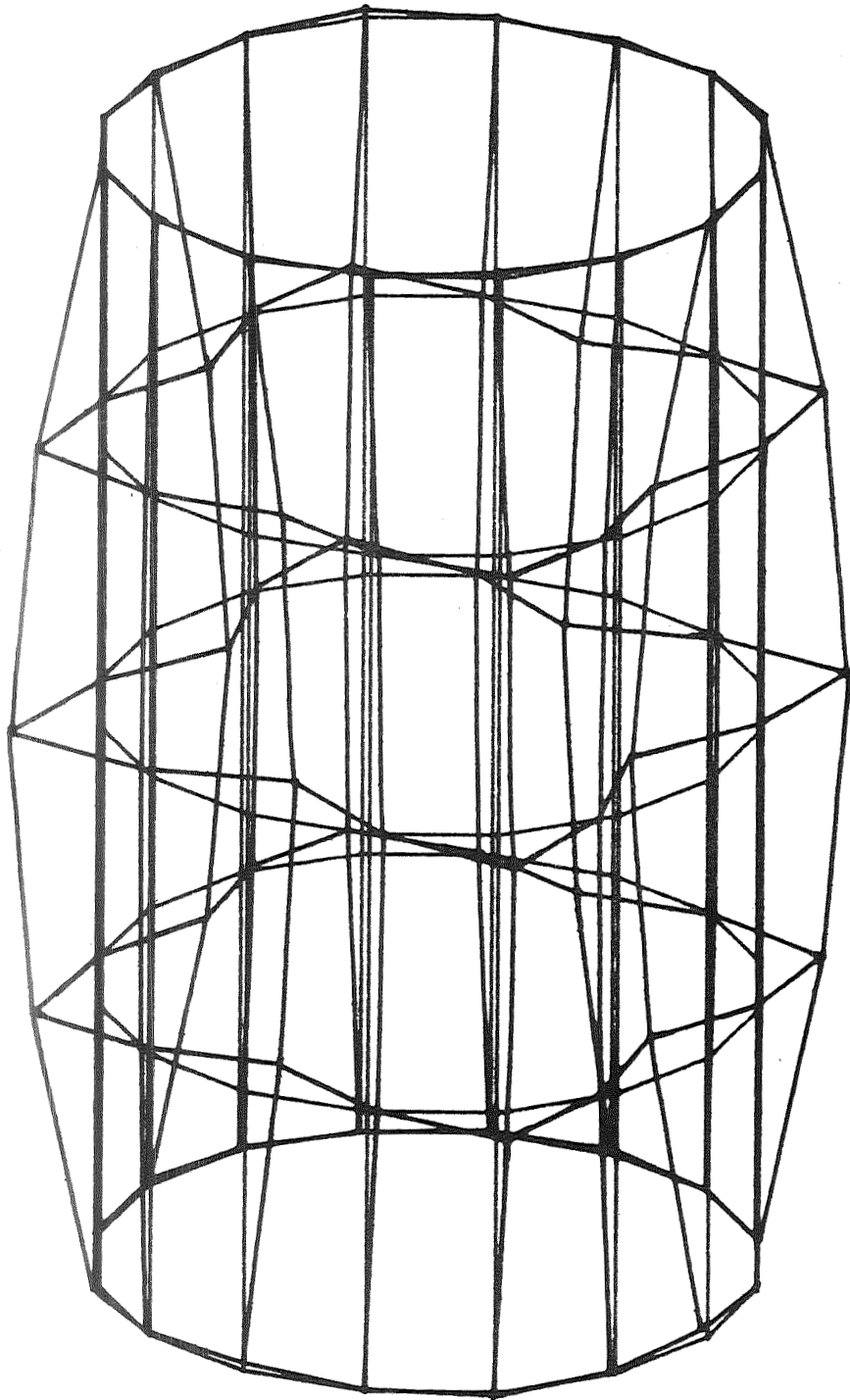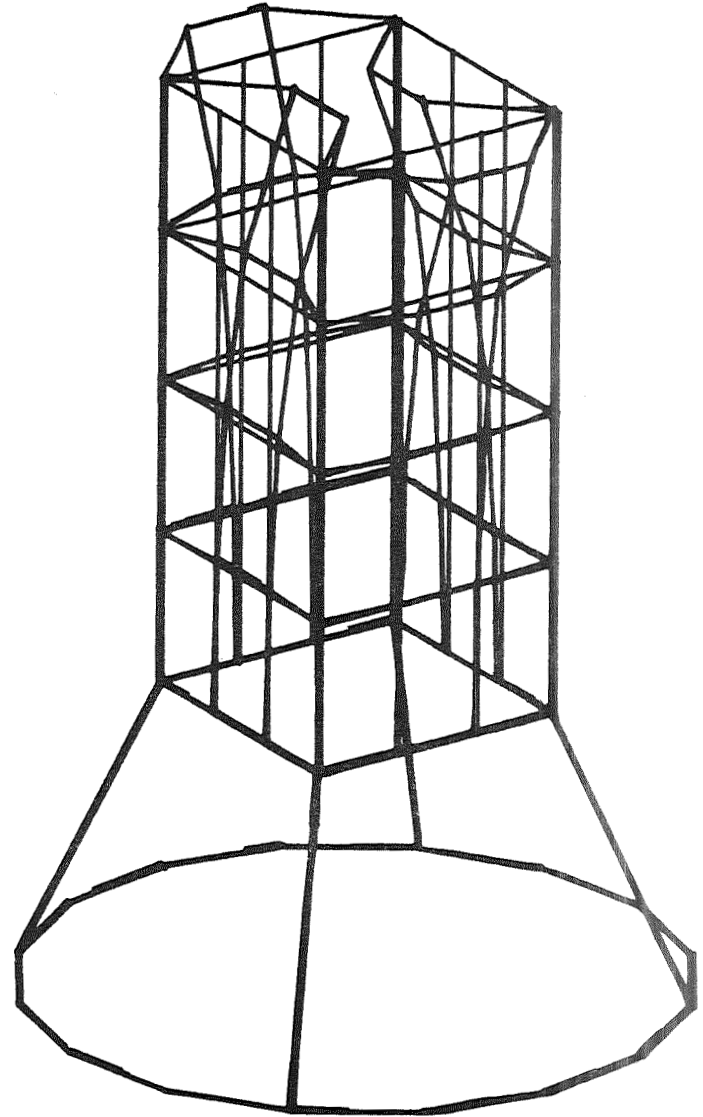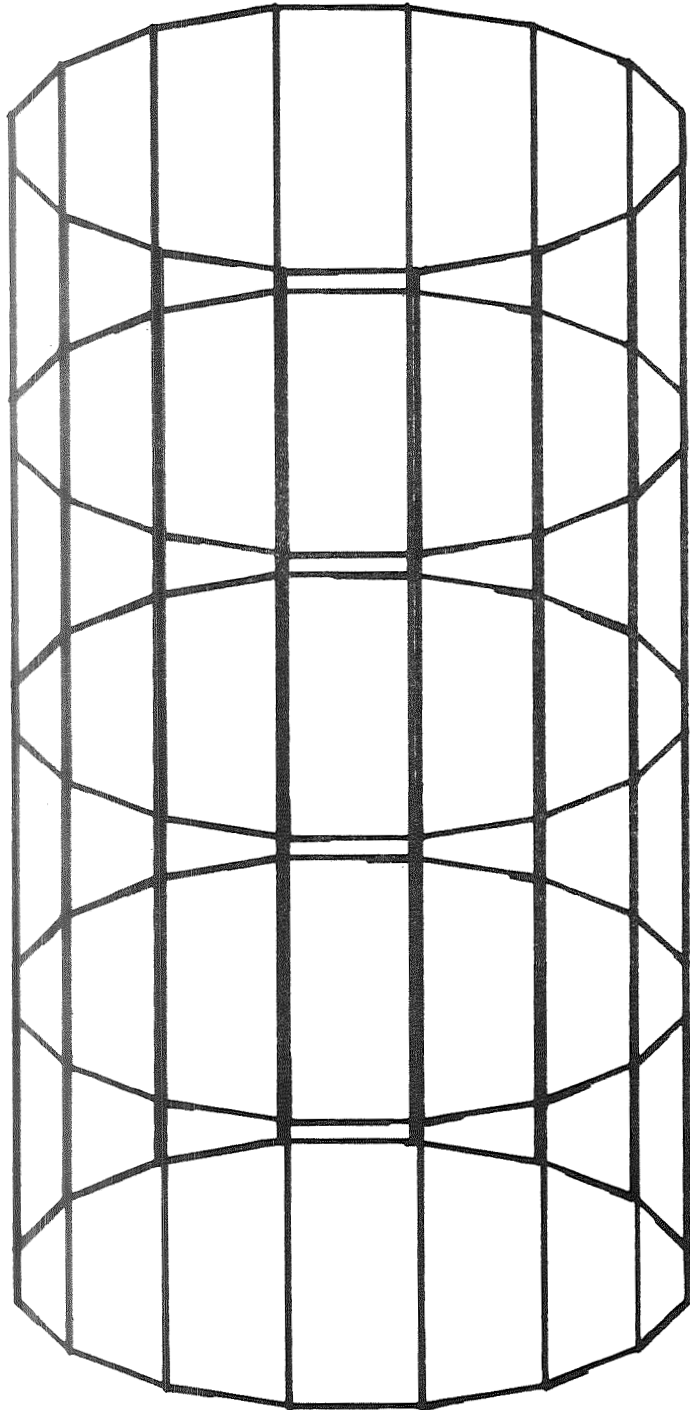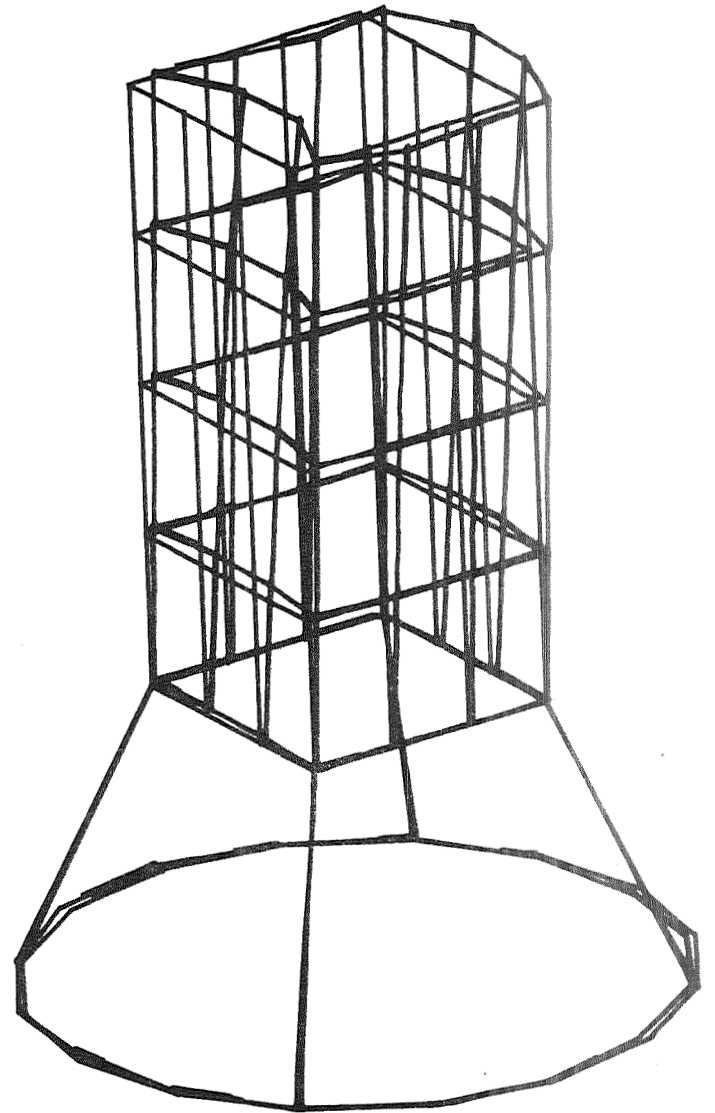
Fig. 3 Mode 10
       Nat. Freq.=61cps
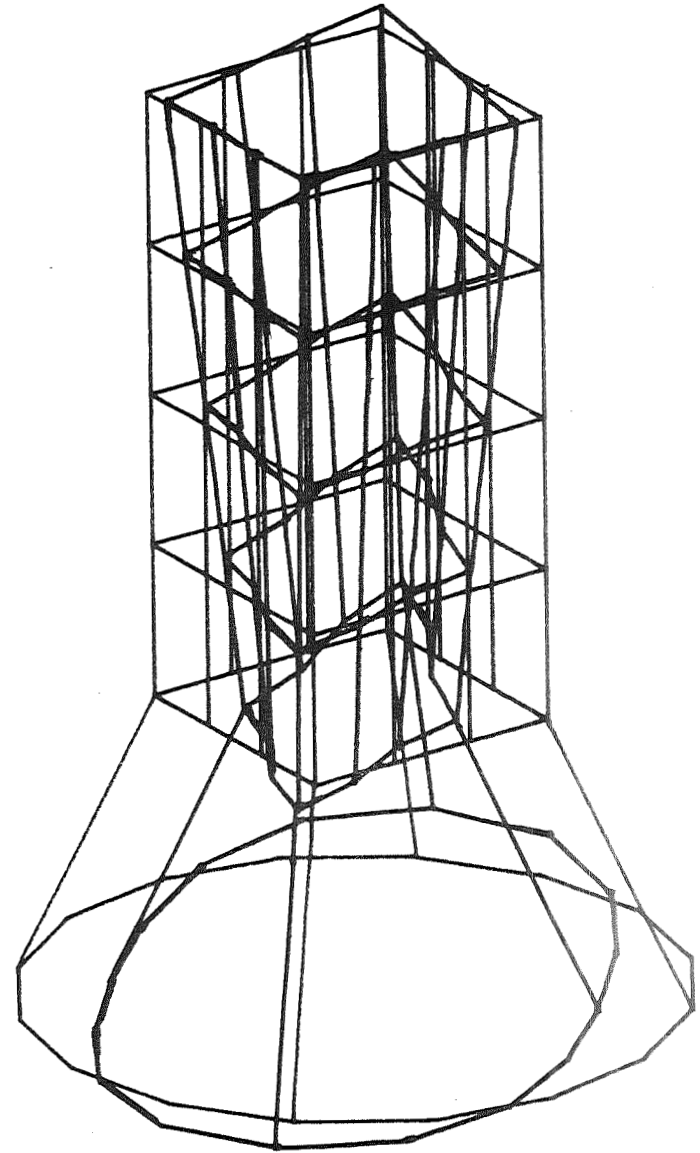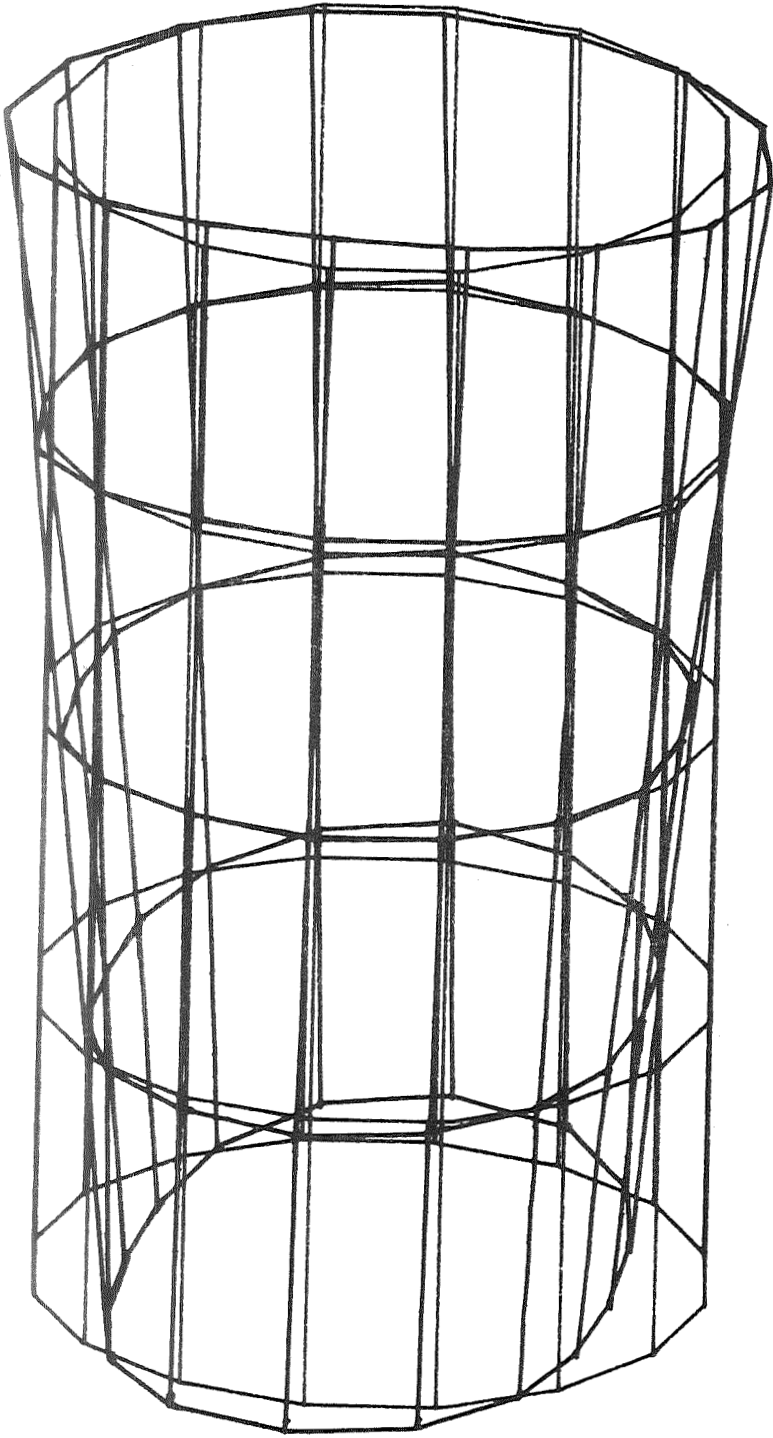
Fig. 4 Mode 11
Nat. Freq.=62cps
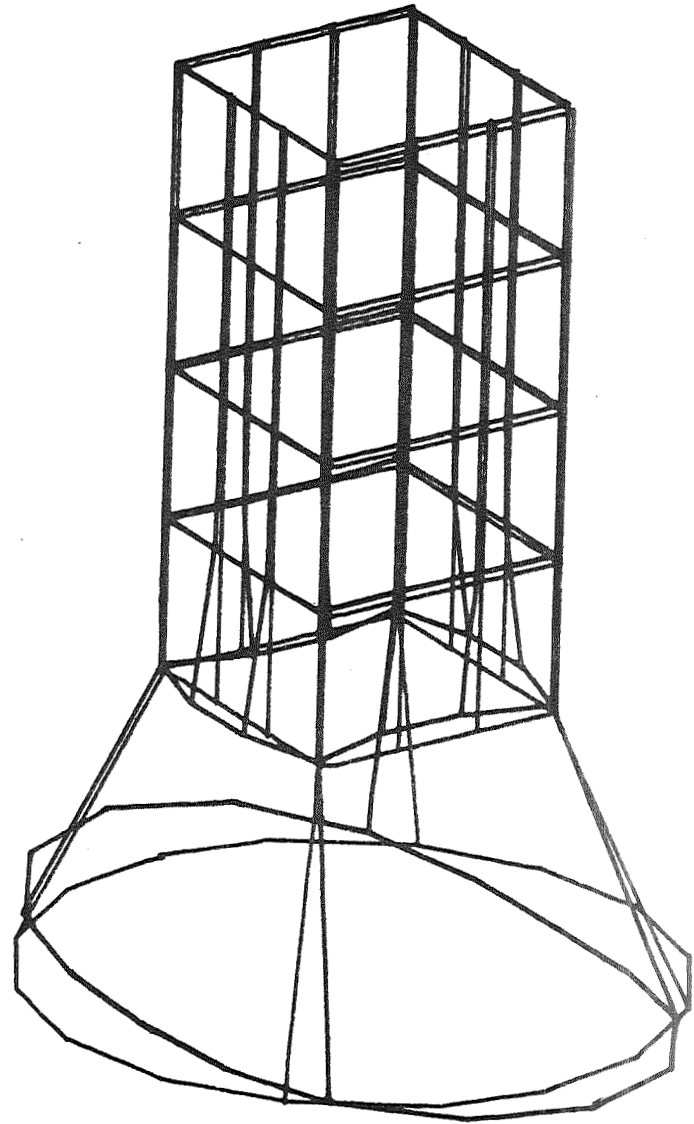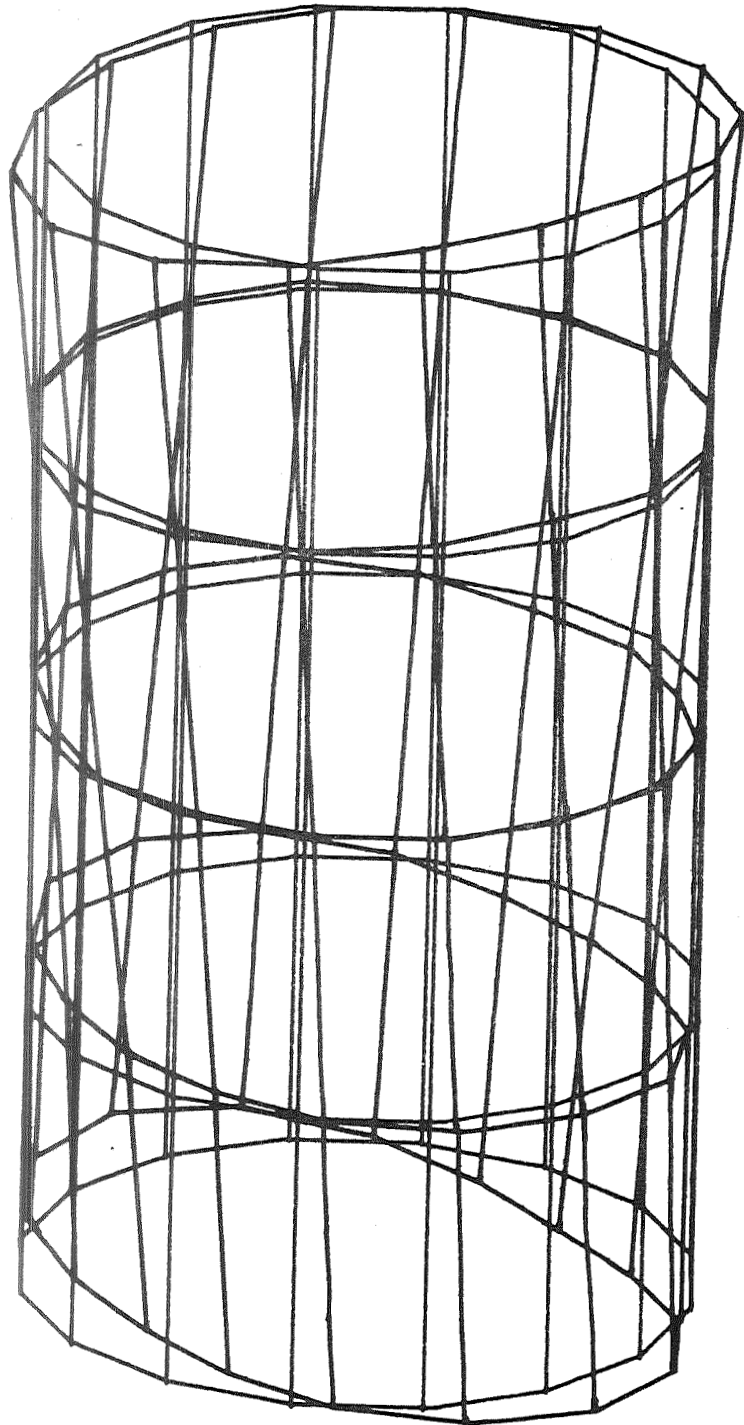
Fig. 5 Mode 13
Nat. Freq.=66cps

33
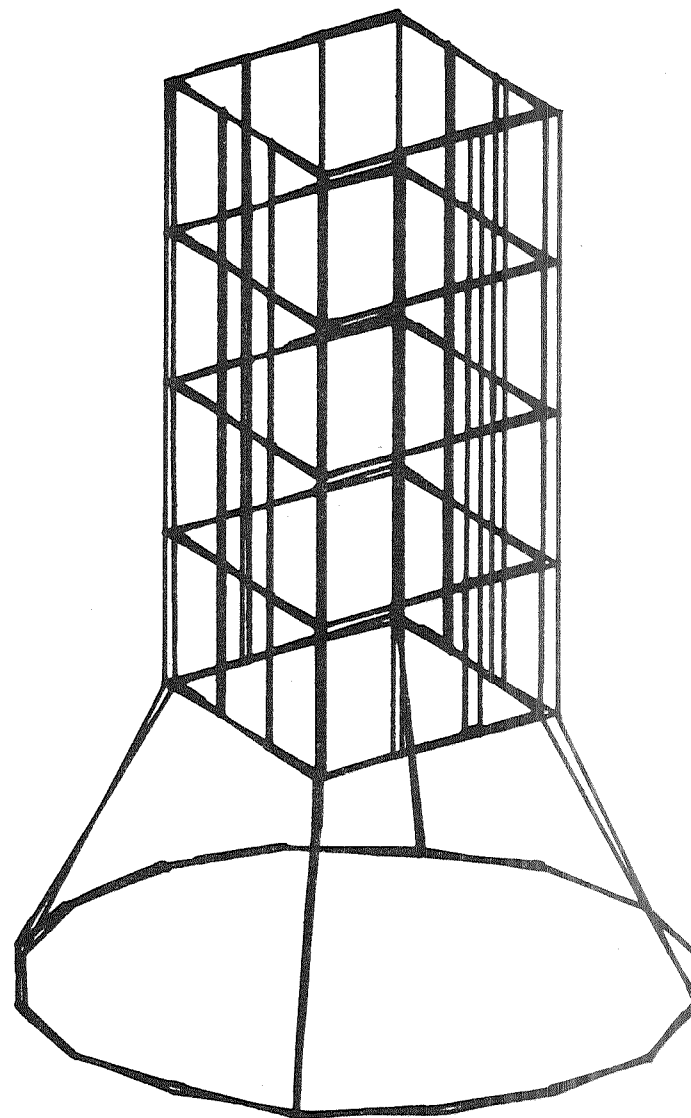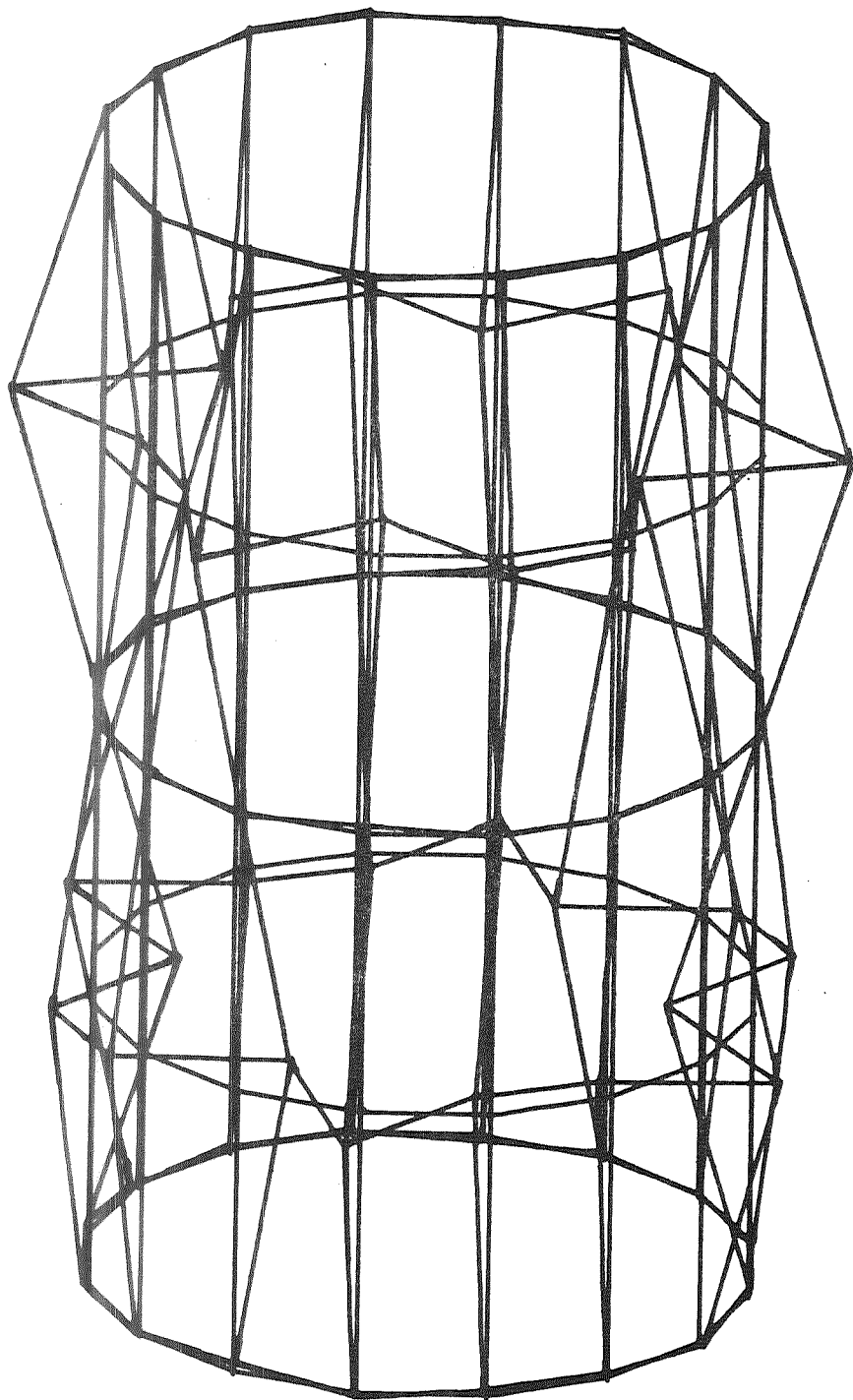
Fig. 6 Mode 25
      Nat. Freq.=141cps

34

Fig. 7 Mode 29
        Nat. Freq.=163cps
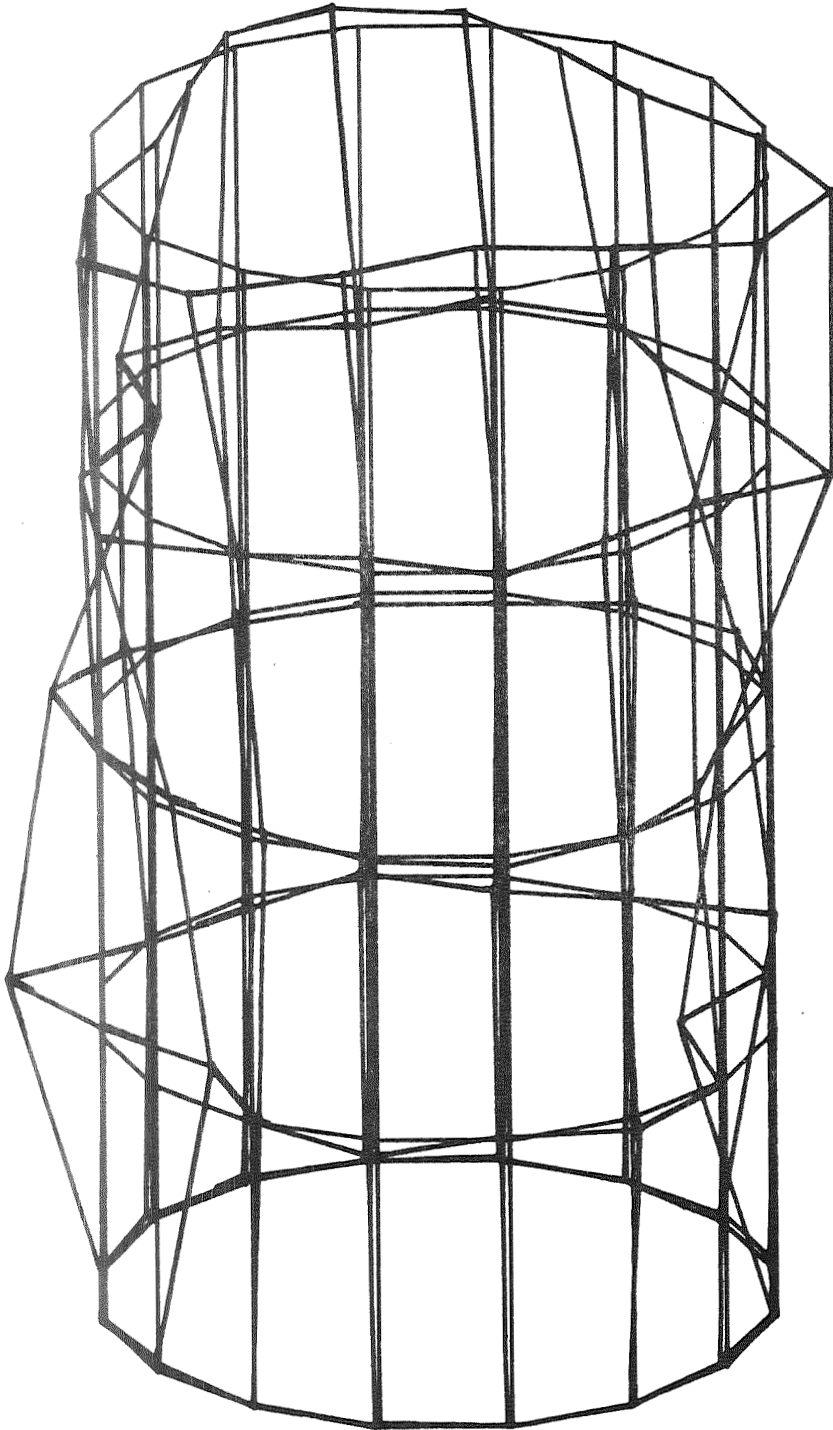
Fig. 8 Mode 30
    Nat. Freq.=173cps
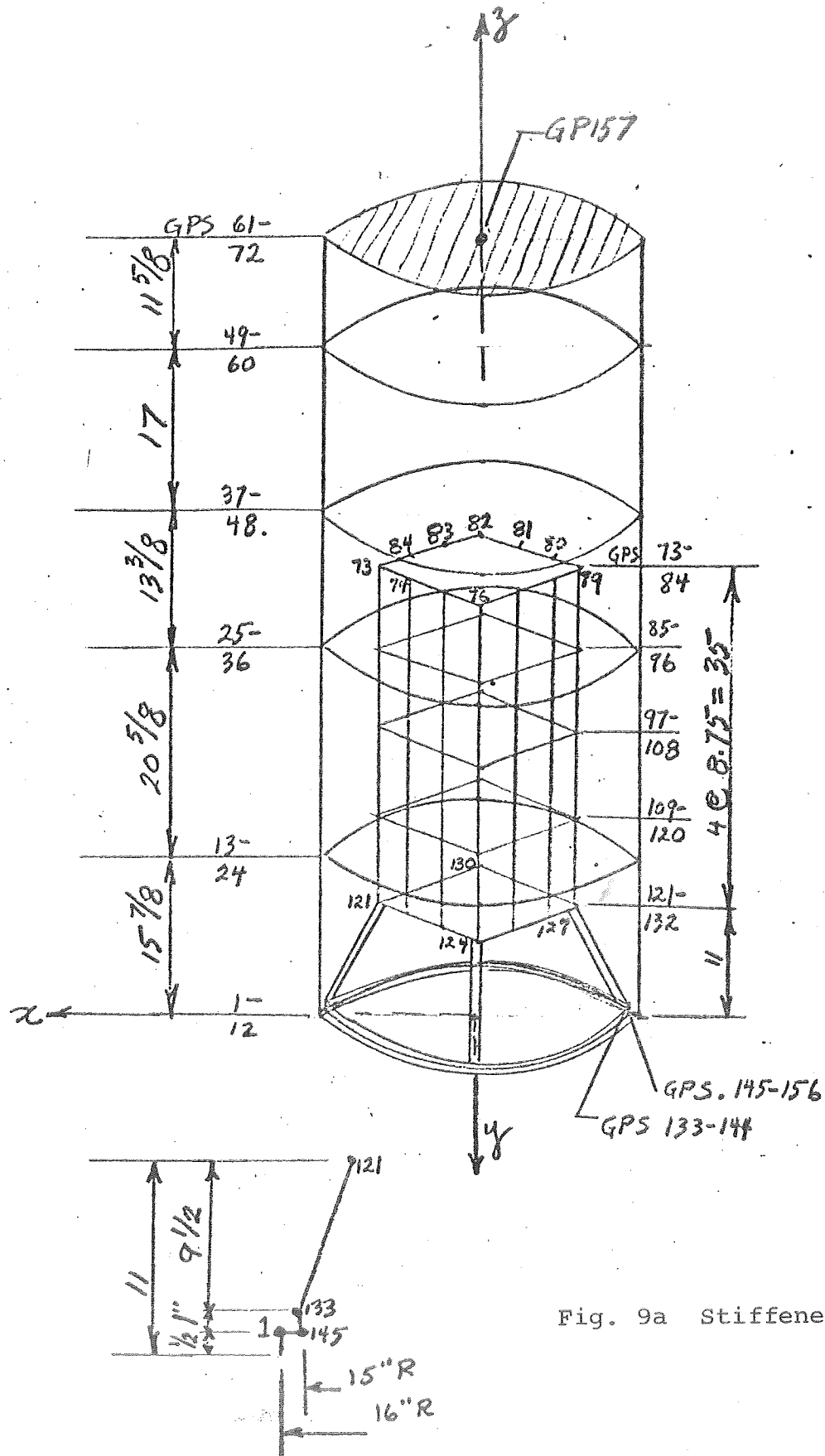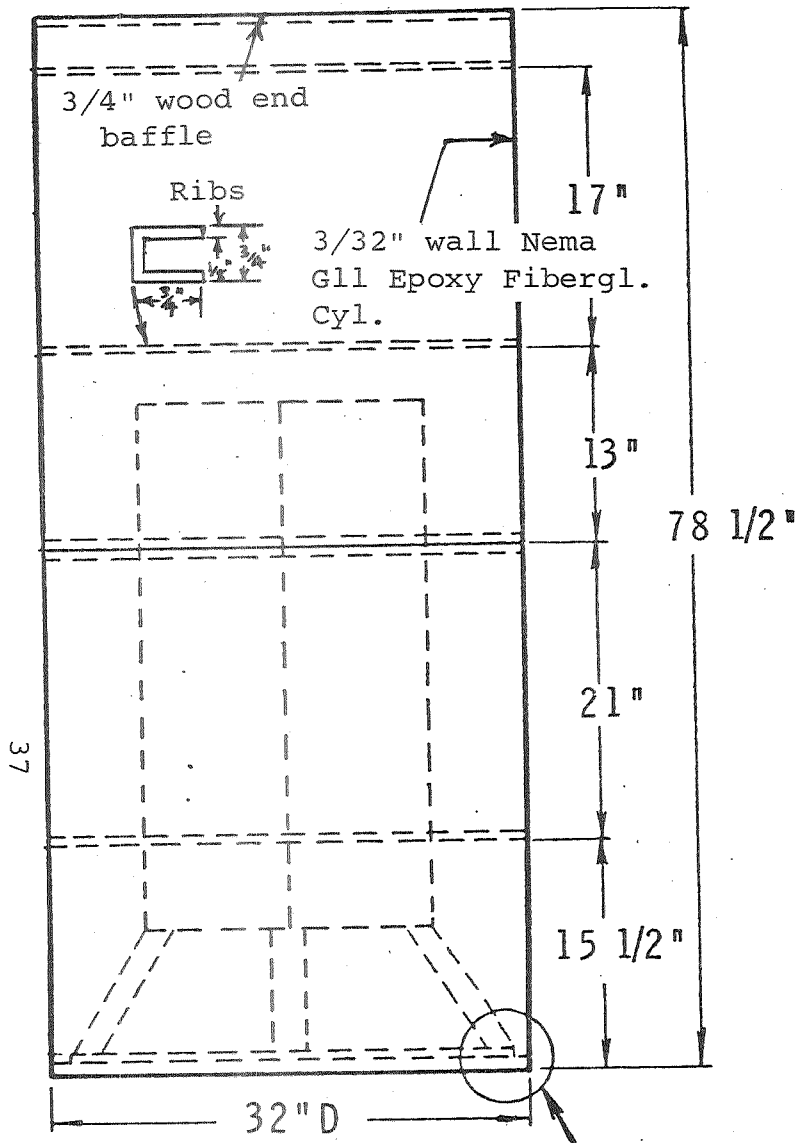
35

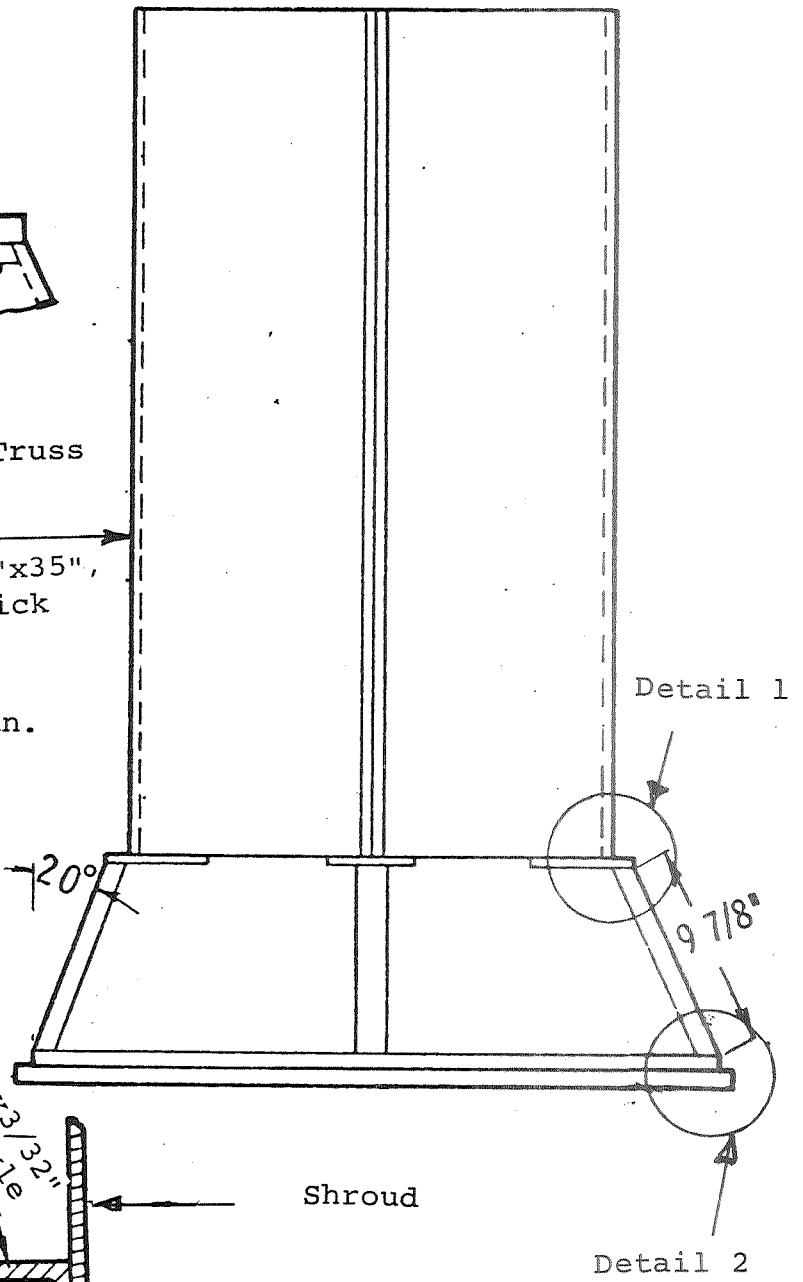Fig. 9a   Stiffened Shroud

3/4" wood end baffle

Ribs

3/32" wall Nema G11 Epoxy Fibergl. Cyl.

17"

13"

78 1/2"

21"

15 1/2"

32" D

Truss 1.5"x1.5"x1/16" Alum. Chan.

Spacecraft Panel

Detail 1

Mounting Truss
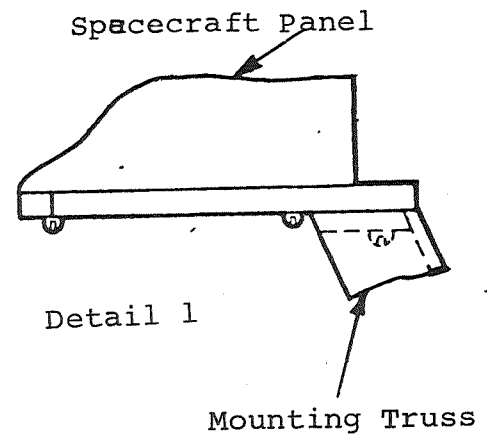
Honeycomb Panels 15"x35", .01" skin, .332" thick

1"x1"x1/8" Alum. Chan.

Truss

1"x1/2"x3/32" Alum. Angle

Ring Frame

15" rad.

16" rad.

Detail 2

20°

9 7/8"
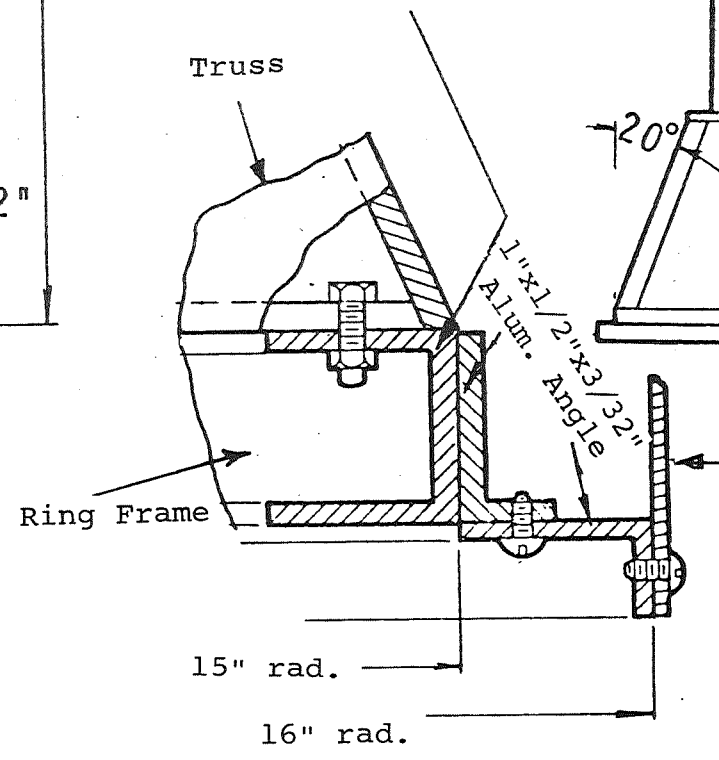
Shroud

Detail 1

Detail 2

Fig. 9b. Stiffened Shroud Details

37